Article (refereed) - postprint

Abd-Elmabod, Sameh K.; Fitch, Alice C.; Zhang, Zhenhua; Ali, Ramadan R.; Jones, Laurence. 2019. **Rapid urbanisation threatens fertile agricultural land and soil carbon in the Nile delta.** *Journal of Environmental Management*, 252, 109668. 12, pp. https://doi.org/10.1016/j.jenvman.2019.109668

This is a post-print version of the following article:

Abd-Elmabod, S.K., Fitch, A.C., Zhanga, Z., Ali, R.R., Jones, L. (in press). Rapid urbanisation threatens fertile agricultural land and soil carbon in the Nile delta. Journal of Environmental Management https://doi.org/10.1016/j.jenvman.2019.109668

The online version can be downloaded here:

https://www.sciencedirect.com/science/article/pii/S0301479719313866?via%3Dihub

Rapid urbanisation threatens fertile agricultural land and soil carbon in the Nile delta

Sameh K. Abd-Elmabod [a,b,c,*], Alice C. Fitch [c], Zhenhua Zhang [a], Ramadan R. Ali [b], Laurence Jones [c]

[a] Institute of Agricultural Resources and Environment, Jiangsu Academy of Agricultural Sciences, Nanjing, 210014, China

[b] Soils and Water Use Department, National Research Centre, Cairo, 12622, Egypt

[c] Centre for Ecology and Hydrology (CEH-Bangor), Environment Centre Wales, Deiniol Road, Bangor, LL57 2UW, UK

Highlights

We quantify rapid urbanisation over four decades in Egypt's Nile delta

Urban sprawl threatens highly fertile cultivated land, and soil carbon stocks

Agriculture expands to less fertile areas, dependent on unsustainable water use

Better management of existing agricultural land has potential to improve soils

Abstract

Agriculture land in Egypt represents only 3.8% of the total area. The Nile delta provides two thirds of Egypt's agriculture land, but is threatened by urban sprawl. The paper aims to quantify urban expansion over a 45 year period using 6 time points from 1972 to 2017, and its impacts on agricultural potential, soil organic carbon stocks, and implications for water use. The study used multi-temporal satellite data and remote sensing techniques (Maximum Likelihood supervised classification, and NDVI), soil sampling and analysis, data on water irrigation, and agroecological system and ecosystem services model (MicroLEIS, InVEST) to assess the effects of land use change.

Urban area increased by a factor of 5, from 452 km^2 in 1972 to 2,644 km^2 in 2017. The greatest losses occurred to the fertile *Vertic Torrifluvent* soils on the older delta, which lost 1,734 km^2. Soil organic carbon (0-75 cm depth) lost as a result of soil sealing from urbanisation rose from 25,000 to 141,000 Mg C over the 45 years. As a result of increased pressure on delta land, agriculture expanded into the higher desert areas outside the delta, on marginal land sustained by intensive fertiliser use and irrigation, which in turn puts pressure on water use. Therefore, rapid urban expansion has resulted in a loss of soil carbon and a shift in agriculture from fertile soils to marginal soils, requiring more capital inputs, which is ultimately less sustainable. Modelling suggested that soil management improvement could make better use of fertile soils within the Delta currently affected by high salinity and poor drainage.

Future planning should encourage urban expansion on the less fertile soils outside of the delta, while improving suitability of existing agricultural land and minimising land degradation within the delta.

Key words: Urban sprawl, soil organic carbon, NDVI, water use, InVEST ecosystem services model

1 Introduction

The world's population is urbanising rapidly. At a global scale, over half of the population now live in cities (UN-Habitat, 2016; Bai et al., 2018; Leeson, 2018; McNabb, 2019). Urban dwellers make up >75% of the population in many industrialised countries, and the size of the urban population in rapidly industrialising countries is also increasing (UNPD 2018). In particular, the rate of change in urban areas can lead to substantial environmental pressures (Fernandes, 2002; Weber and Puissant, 2003; Sudmeier-Rieux et al., 2015; Li et al. 2019).

Globally, the effects of urban sprawl on agricultural areas are increasingly recognised, with impacts on food security (Deng et al., 2006; Long et al., 2018; Gomes et al., 2019; Zhou, et al., 2019), regional climate (Carlson and Arthur, 2000; Shastri and Ghosh 2019), hydrology (Weber et al., 2001; Haase and Nuissl, 2007) and biodiversity (Crist et al., 2000; Concepción et al., 2015). The direct pressures caused by urbanisation are usually localised around cities themselves (Bugnot et al., 219; Liu et al., 2019). Key among these is the direct loss of land through construction of buildings and infrastructure, and an associated loss of the ecosystem services provided by soil natural capital, such as carbon storage and food production (Cui et al., 2019; García-Nieto, et al., 2019; Wang et al., 2019; Wen et al., 2019). A further consequence of urbanisation is that agricultural production is displaced, often to less suitable areas, requiring more resource inputs such as increased use of fertiliser and irrigation water (Rizvi, et al., 2018; Umesha et al., 2018). There has been a recent focus on the effects of urbanisation on soil-related services, particularly soil carbon. Urban soils are typically low in carbon, and comprise highly disturbed soils containing much man-made material from construction, and often very compacted (De Kimpe & Morel, 2000). In the US, Lavy et al. (2016) studied impacts of urban sprawl, showing mixed impacts on soil carbon. In China, Li et al. (2018) and He et al. (2016) both showed large scale carbon loss due to urban expansion of Xuzhou City and Beijing respectively. However, in Moscow a modelling study estimated potential increases in urban soil carbon resulting from high carbon storage in areas of urban greenspace (Vasenev et al. 2018). In Egypt, urbanisation has led to a decrease in soil organic carbon in the top soil by 285.4 Mg C ha^{-1} in the Tanta Catchment in the northern part of Nile delta (Abu-hashim et al., 2016).

The Nile delta in Egypt is a useful case study in which to investigate this nexus. The delta is geographically constrained and is experiencing high population pressure on its natural resources. Egypt has a land area of 1.01 million km^2, and a total population of ~100 million inhabitants. However, since much of the country is desert both urban and agriculture areas are concentrated in the Nile valley and the delta. Together these comprise only 4% of the total area of Egypt (CAMPAS, 2017). During the last forty years, Egypt's population has almost tripled, from 36.6 million in 1972 to 97.5 million in 2017. The expansion of towns and villages dotted around the delta has resulted in rapid

urbanisation (Shalaby and Moghanm, 2015), leading to unprecedented pressure on the fertile agricultural land of the Nile delta. As a result, the available area per capita in the delta has dropped from 0.12 ha in 1950 to 0.04 ha in 2017 (CAPMAS, 2017), and there is concern that urban encroachment on fertile and highly productive soils may threaten Egypt's agriculture sustainability and food security (Nizeyimana, 2001). The delta is the main agricultural area of Egypt, comprising around 64% of the total agriculture land area. It produces about two thirds of Egyptian crop production (FAOSTAT, 2018, www.fao.org/faostat/en/), and the fertile soils allow two or three crops to be grown per year (Osama et al., 2017; Kassim et al., 2018). While, the Egyptian crop lands are 100% irrigated as a lack of precipitation and high evapotranspiration, the intensive irrigation under arid climate represents the main reason of the salinization problem practicality in the old cultivated land (Kotb et al., 2000). Salinity and poor drainage negatively affect the crop production and agriculture sustainability (Maas and Grattan 1999; Manik et al., 2019; Zörb et al., 2019).

Previous studies on urbanisation and land use change in Egypt, have looked at effects of urbanisation on relatively small areas (Shalaby and Tateishi, 2007; El-Kawy et al., 2011; Hegazy and Kaloop, 2015; Ezzeldin et al., 2016), or discussed remote sensing methods for land use change detection (Dewidar, 2004; Shalaby and Tateishi, 2007). Two studies have assessed impacts of urbanisation across the whole delta region. Sultan et al. (1999) looked at urban change over three decades (1972-1990) and the implications for loss of agricultural land, while Shalaby (2012) looked at three time periods (1984, 1992 and 2006) and discussed urban sprawl across soil types and land capability classes. Both these studies highlighted rapid loss of agricultural land but did not report on loss of soil carbon or assess potential policy responses to mitigate this loss. Assessing the wider consequences of land use change on surrounding areas is essential to understand sustainability in a land use context. This assessment process can make use of a range of techniques, including remote sensing and models. Remote sensing data can play a vital role in monitoring land cover change over time (Grădinaru et al., 2019; Zhang et al., 2019), while remote sensing products such as NDVI are useful for monitoring vegetation and crop coverage (Nageswara et al., 2005; Yang et al., 2010; Park et al., 2016; Han et al., 2019).

Agroecological models such as the Micro Land Evaluation Information System (De la Rosa et al., 1992; 2004; 2009) evaluate the agricultural land potential, based on soil physical and chemical parameters, slope and climatic factors. Soil management techniques have the potential to alleviate some of these factors and therefore to increase the agricultural suitability of certain soils (Abd-Elmabod et al., 2019). Meanwhile, ecosystem service models such as InVEST (Nelson et al., 2009) allow rapid assessment of carbon stocks. These models tend to rely on parameters provided in default look-up tables, or on values derived from the literature. Yet the accuracy of these models can be considerably improved by

the use of local or national data to tailor them to a specific context (Sharps et al., 2017; Redhead et al., 2017; Liu et al., 2019), for example, by using local measurements of soil carbon stock.

In summary, previous studies have tended to focus on land use change in small parts of the Nile delta, not across the whole extent. They have not assessed carbon stocks, and have not addressed land use change in a holistic manner, including soil quality, agriculture and water use. Therefore, this paper aims to: i) quantify the spatiotemporal dynamics of urban sprawl across the whole Nile delta of Egypt at six time points over four and a half decades (1972, 1984, 1992, 2003, 2011 and 2017), providing a detailed picture of change over time in this highly pressured region, ii) evaluate the impacts of rapid urbanisation on soil carbon stocks, agricultural potential, and water use using a combination of models, remote sensing techniques, field data and national statistics, iii) evaluate the potential to improve agricultural productivity on the older delta soils using scenarios of agricultural soil management, and to draw out the resulting implications for agricultural production.

2 Material and methods

2.1 Study area description

The study area (**Fig. 1**) focuses on the Nile delta and immediate surrounding area, in the north of Egypt at coordinates 30° 01' - 31° 36' N and 29° 39' - 32° 29' E. It includes 13 provinces: Cairo, Alexandria, Suez, Port Said, Dumiat, Dakahlia, Sharqia, Qalyubia, Kafr El Sheikh, Gharbia, Monufia, Beheira, Ismailia (lower Egypt region) and a small part of Giza province (from middle Egypt). The River Nile divides north of Cairo into two main branches Rashid and Damietta. The delta lies between and alongside these two branches of the Nile.

<Fig. 1>

The elevation of the Nile delta ranges from -11 to 20 m above sea level and has a flat topography. The surrounding areas are mainly higher elevation, reaching up to 713 m, but also include a low-lying depression (-30 m) in a small area in the western part of the studied area (**Fig. S1A**). The dominant soil groups are *Aridisol* and *Entisol*. The dominant soil subgroup is the *Vertic Torrifluvent* that covers 29% of the studied area, illustrated in **Fig. S1B** (Soil Survey Staff, 2014). The soil units of the Nile delta were adapted from the soil map of Egypt (ASRT, 2009), using the soil classification of USDA (2014). Poor drainage and salinization are the major limiting factors for agriculture sustainability in Nile Delta (Abdel-Dayem, 1990; Kotb et al., 2000; Mohamedin et al., 2010), about 60 % of the total cultivated land of the Nile Delta are salt-affected soils (Aboukhaled et al., 1975; Kotb et al., 2000). The soil types *Typic Haplosalids, Aquic Torrifluvent, Typic Torrifluvent* and *Vertic Torrifluvent* are the most impacted soils with salinization and poor drainage problems The land originally cultivated in the Nile delta lies on the flatter ground of the main Delta. It is a fluvial soil that formed through Nile silt formation, where

149 the deposition of Nile silt was 0.9 mm/year and the depth of the deposited silt ranges from 8.5 m to
150 11.3 m (Ball, 1939). That means a layer with 10 m depth has been formed over a duration of 10
151 thousand years. For the purposes of this paper, we considered the agriculture land in 1972 as 'old
152 cultivated land', while any increase in the agriculture area in the other studied dates is considered as
153 'new cultivated land', which lies primarily in the hillier areas to the west and outside of the delta. The
154 area is extremely arid, with annual precipitation < 200 mm. In the last five years, the mean total annual
155 precipitation at the Cairo metrological station was 15.4 mm, and was 166 mm at the Alexandria station
156 (CLAC, 2016).

157 A wide range of crops are grown, mainly in small fields, with the average size of a field unit being only
158 1.05 ha. In Egypt, there are three cropping seasons for annual crops: winter (cultivated from
159 September-November), summer (cultivated from February - May) and Nili (cultivated from July-
160 August). Fruits/orchard crops are also cultivated. The major winter crops are wheat, barley, beans,
161 sugar beet, onion, garlic, flax, lupine, clover and vegetables. Summer crops are cotton, maize,
162 sorghum, rice, sunflower, sugarcane, onion, sesame, soybean and vegetables. Nili crops are maize,
163 sorghum, rice, sunflower, onion and vegetables (CAMPAS, 2017). **Fig. S1C** shows land cover within the
164 studied area (CCI Land Cover – S2 Prototype Land Cover 20m Map of Africa 2016).

165 Agriculture constitutes 81.6 % of Egypt's water use and due to the low rainfall, irrigation water from
166 a range of sources is an essential component of Egypt's agricultural production. Annual water use in
167 Egypt is 76.4 billion m^3 (CAMPAS, 2017). The River Nile provides 73% of this requirement (55 billion
168 m^3 per year), 6.9 billion m^3 (9 %) comes from groundwater in the Nile valley and delta, and 11.7 billion
169 m^3 from the re-use of sewage water (15%) (CAMPAS, 2017). **Fig. S1D** illustrates the distribution of the
170 irrigation and drainage canals through the studied area (ASRT, 2009). Reclaiming new agricultural land
171 requires substantial irrigation water, and this may not be sustainable. Use of groundwater in particular
172 is not sustainable since rates of groundwater use are far higher than rates of natural recharge. The
173 management scenarios used in this study aim to explore improvement of the capability and
174 productivity of the original old cultivated areas, which do not require additional irrigation water.

175 **2.2 Quantifying urban sprawl and agriculture areas over time**

176 The assessment approach considers changes in land use and its implications on soil natural capital and
177 associated resource use. **Fig. S2.** illustrates a general schematic diagram of the overall methodology.

178

2.2.1 Changes in land cover over time

Remote sensing satellite data were used to classify changes in urban extent and agricultural area over time. In this study, multi-temporal satellite images of Landsat were used. These data include Multispectral Scanner (MSS) acquired in 1972, Landsat Thematic Mapper (TM) acquired in 1984 and 1992, Landsat Enhanced Thematic Mapper Plus (ETM+) acquired in 2003 and 2011 and Operational Land Imager (OLI) acquired in 2017 (see **Tables S1**, **S2** and **S3** for full details).

Geometric correction was carried out using ENVI 5.0 software (Exelis VIS, Boulder, CO), dependent on ground control points from topographic maps to geocode the images acquired during 1972. The Landsat ETM+ scan line corrector (SLC) failed on May, 2003, causing scan gaps. The ETM+ continued to acquire data with the SLC powered off, leading to images that are missing approximately 22 % of the normal scene area. To improve the utility of the SLC-off images (acquired in 2003 and 2011), the original SLC-off images have been replaced with estimated values based on histogram-matched scenes. The image was calibrated to radiance using the inputs of image type, acquisition date and time, then it was stretched using linear 2%, smoothly filtered, and the histograms were matched (Lillesand and Kiefer, 2007). Atmospheric correction for ETM+ images was done using FLAASH module (ITT, 2009). The images were radiometrically rectified and the reflectance of all images was derived using ENVI 5.0 software.

Land cover types are normally mapped from remotely sensed data using a supervised digital image classification (Campbell, 2011; Thomas et al., 1987). In this study supervised classification (maximum likelihood) was done using ground check-points and topographic maps of the study area. The overall accuracy and kappa coefficient of the classified images were calculated by comparing classified data with 1200 reference points for each studied date. The accuracy (Table S4) exceeds recommendations by Anderson et al. (1976) and Thomlinson et al. (1999) that land use/land cover mapping accuracy using Landsat data should be greater than 85% and no single classified class less than 70%.

2.2.2 Annual Urban Expansion Rate

The annual urban expansion rate (UER) was calculated according to Ma and Xu, (2002) and Xiao et al. (2006), to investigate the rate of urban sprawl over the studied periods, which can be calculated as illustrated in **Eq. 1**

$$UER_{\text{n to n+i}} = \frac{BuA_{\text{n+i}} - BuA_{\text{n}}}{i} \qquad \textbf{(Eq. 1)}$$

where UER_n to $_{n+i}$ represent the annual UER from the year *n* to the year *n + i*; BuA_n and BuA_{n+i} are the total built-up area at the time of year *n* and year *n + i*, respectively. Values show the increase in urban area per year.

2.2.3 Normalized Difference Vegetation Index (NDVI)

We used NDVI (GeoSpatial Analysis 5th Edition, 2018; Park et al., 2016) to evaluate seasonal patterns of land cover and the fertility and land use of delta land. NDVI values range from –1 to 1 (Burgan and Hartford, 1993). The NDVI calculation output represent an intermediate processing step, whereas four seasonal images during 2017 and 2018 were used to calculate maximum NDVI, i) as input data to the supervised classification for mapping soil carbon, and ii) to identify the most productive agricultural areas in the Land Capability Assessment.

2.3 Soil Organic Carbon

Soil data was obtained for one hundred sixty-eight sampling locations. Seventy one were obtained from field work conducted for this study and ninety seven were selected from another study (Ali, 2003 and ASRT, 2009). These soil samples were selected to be representative of the soil types and land cover classes across the Nile delta, and to achieve good spatial coverage across the study area. Soils in dry regions change relatively slowly, therefore any seasonal and temporal differences between the two soils datasets are assumed to be much smaller than differences between soil types. The location of soil samples are illustrated in Fig S1B. At each location, soils were sampled at depths (0-25, 25-50 and 50-75 cm), air-dried (48 h at room conditions) and sieved (2 mm) before analysis. For each soil depth, soil organic carbon (SOC) was determined by the acid-dichromate potassium and titration method (Walkley and Black, 1934); soil bulk density was determined by the core method (Blake and Hartge, 1986), and soil texture was determined using the pipette method (Kilmer and Alexander, 1949). Subsequently, for each of the sampled soil depths (0-25, 25-50 and 50-75 cm) of the 168 soil profiles, soil organic carbon content (SOCC) was calculated as follows (**Eq. 2**):

$$SOCC = SOC \times BD \times D \times (1-G) \quad \text{(Eq. 2)}$$

Where SOCC is soil organic carbon content (Mg ha^{-1}), SOC is soil organic carbon percentage (g 100^{-1} g^{-1}), BD is bulk density (g cm^{-3}), D is the thickness of the studied layer (cm) and G is the proportion in volume of coarse mineral fragments (>2mm).

Several methods were trialled for mapping soil carbon, following a similar approach to that used in the InVEST ecosystem service modelling tool, where land cover classes or other spatial classifications are assigned carbon values (Nelson et al., 2009). In this study, the collected soils data were used to provide soils data for land cover units. The allocation process included a supervised classification in

ArcGIS 10.4 using land cover, NDVI and soil types as inputs, however, the supervised classification was found to be dominated by soil type. Therefore, the final approach used only soil type to map soil carbon, with an overlay of urban extent in 2017 to screen out sealed areas. Soil carbon values were averaged by soil class. The look-up table providing soil carbon values and carbon density in megagrams per hectare (Mg/ha), by depth for each soil type is provided in Supplementary Material (**Table S5**).

We used the annual cumulative SOC loss rate due to urbanisation (CLR), to investigate the rate of SOC loss over the studied urbanisation periods, as shown in **Eq. 3**

$$CLR_{\text{n to n+i}} = \frac{CL_{\text{n+i}} - CL_{\text{n}}}{i} \qquad \textbf{(Eq. 3)}$$

where, CLR_{n} to $_{\text{n+i}}$ represent the annual CLR from the year *n* to the year *n + i*; CL_{n} and $CL_{\text{n+i}}$ are the total carbon cumulative loss at the time of year *n* and year *n + i*, respectively.

2.4 Land capability evaluation

Maximum annual NDVI together with the assessment results of the land capability model, were used to produce the land capability maps (**Fig. 2**).

2.4.1 Cervatana model for land capability

Land capability assessment was carried out using the Cervatana module of MicroLEIS DSS, with additional data from NDVI images, soil maps and land evaluation. This information was brought together to map and assess agricultural land capability in the studied area. The MicroLEIS DSS is a decision support system developed to assist decision-makers facing specific agro-ecological problems (De la Rosa et al., 2004). The Cervatana module evaluates the general land use capability or suitability for agricultural use. Cervatana computes different groups of variables (topography, soil properties, erosion risk, and bioclimatic deficiency; and provides a classification of agricultural suitability (**Fig. S3**). The four broad classes resulting from the Cervatana land capability module are: 1- **Optimum class**, where the classified land has the highest agricultural quality, excellent productivity and a very good natural fertility, and with very few limitations restricting its use for a wide range of cultivation crops, under appropriate management; 2- **Good class**, with good productivity under appropriate management, but it may have topographic, edaphic and/or climatic limitations which reduce the set of possible crops and the productive capability; 3- **Moderate class**, has considerable limitations related to topographic, edaphic, and /or climatic factors and therefore has a smaller range of possible cultivation crops, it also needs appropriate conservation practices to maintain continued productivity;

4-**Marginal class**, is totally non-productive, lacks the essential ecological conditions for agricultural crops, and requires intensive management and conservation practices to be of agricultural benefit. The calculations within Cervatana are empirically-based, formulated and calibrated using expert knowledge. (De la Rosa et al., 1981, 1992; Anaya-Romero et al., 2015). In this application, the Cervatana model allocates individual soil samples to a land capability class, based on their soil chemistry and physical properties. Therefore, mapping land capability was based on the spatial data (i.e. Cervatana outputs of one hundred sixty-eight sampling locations, maximum annual NDVI, soil map and digital elevation model).

2.4.2 Soil management scenarios

Two scenarios were considered: a baseline of soils in their current condition (in 2017), and an alternative scenario where agricultural potential is improved through a range of soil management techniques, described below. The Cervatana model was run under the current situation to assess current land capability evaluation. The major soil limiting factors for the land capability are texture, soil depth, drainage and salinity (Abd-Elmabod et al., 2017). Soil depth and texture are inherent soil characteristics and are not easily modified or amended (Abd-Elmabod et al., 2017). Therefore, in the improvement scenario two manageable soil factors were considered as options to improve land capability: soil salinity and drainage (Abd-Elmabod et al., 2019). For both these factors, management options exist which allow improvement in their characteristics. In this scenario, the soils with the potential to improve were soils that have salinity values less than 16 dSm^{-1}, achieved by the use of soil flushing. The recommended improvement is to reduce the salinity to 3 dSm^{-1} (Abd-Elmabod et al., 2019). Drainage can be improved by the installation of field drains. This can lead to an improvement from the classes: 'very poor', 'poor', or 'imperfect' to the class of 'good' status (De la Rosa et al., 1982; Abrol et al., 1988; Abd-Elmabod et al., 2019).

2.5 Water use

Annual water consumption for irrigation, by crop type and by Province for 2015, was collated from The Central Agency for Public Mobilization and Statistics (CAPMAS, 2017) from its annual bulletin on Irrigation and Water Resource statistics. Comparable data on water use for previous time periods was not readily available.

3 Results

3.1 Urban Expansion, 1972 - 2017

Since 1972, the urban area in the delta has increased more than five-fold, from 452 km^2 in 1972 to over 2,600 km^2 in 2017(**Fig. 2 and Fig. S4**). The rate of change increased dramatically after 2003, with

the population increasing from 19 million to 55 million (**Fig. S4**). The spatial pattern of expansion (**Fig. 2**) shows that this is driven by an increase in both small and large settlements, spread fairly uniformly across the delta area and is not just a result of expansion of Cairo in the south of the delta. Urban expansion has occurred primarily on the older agricultural areas and avoids the higher elevation hilly and drier areas (**Fig. S1A**). **Fig. S5** illustrates the main land cover types in Nile delta.

<Fig. 2>

Table S6 shows the urban expansion rate (UER) per year, while **Table 1** breaks down the urban expansion by soil type over the six time points. Vertic Torrifluvents are one of the most fertile soil types in Egypt, and by far the greatest loss in area was due to urban expansion on this soil type, with a third of that loss (354 km^2) occurring in the years since 2011. The UER for this period was 59 km^2 yr^{-1}. This represents a major loss in agricultural production potential. Low fertility soils like the *Typic Haplosalids* and *Typic Petrogypsids*, and the *Typic Quartzipsamments*, *Typic Torripsamments, Typic Torriorthents* and *Typic Haplocalcids* which surround the Nile delta have a low urbanisation rate, despite covering about 30 % of the studied area (12146 km^2).

<Table 1>

3.2 NDVI

Fig. 3 illustrates how NDVI values change over time in four different months during 2017 and 2018. The signal from water bodies occupies the lowest NDVI values (-0.5 - 0.0), bare land and urban occupy low values (0 - 0.1), while the higher NDVI values reflect natural vegetation and cropland where the values ranges from 0.1 - 0.7 (Demirel et al., 2010; Zhang et al., 2009; Wang et al., 2019).

In October, farmers are preparing the farmland, sowing and planting the winter crops; for this reason, the majority of the agriculture land has low NDVI values compared with values in February where the winter crops are fully grown. Following the same trend, the summer crops are cultivated from February – May, thus the NDVI values are low in May compared with July.

<Fig. 3>

3.3 Soil Carbon Stocks in the Nile delta

The highest SOC stocks in delta soils (0-75 cm depth) are located in the northern parts of the Nile delta, where SOC values reached 106 Mg ha^{-1} in the soil type *Aquic Torrifluvents*, 101 Mg ha^{-1} in *Typic Torrifluvents* and 94 Mg ha^{-1} in the *Typic Aquisalids*. The dominant soil type *Vertic Torrifluvents* also has a high SOC content of 72 Mg ha^{-1}. Much lower values of SOC are in *Typic Petrogypsids* (17 Mg ha^{-1}) and *Typic Torripsamments* (25 Mg ha^{-1}) (**Fig. 4A**, and **Table S7**). Carbon density is fairly high in the

fertile *Vertic Torrifluvents* soils (0.0123 gC cm^{-3}), but much lower in the sandy desert *Quartzipsamments* soils (0.0067 gC cm^{-3}). The top 25 cm generally holds the most carbon, but all soil types show that carbon is stored at all three depths, including in the more fertile *Vertic Torrifluvents*.

Since urban expansion has primarily occurred on the most fertile soil types, which also hold the most carbon, there has been considerable loss of soil carbon due to urbanisation. The cumulative loss of SOC for three soil depths (0-25, 25-50 and 50-75 cm) is shown in (**Fig. 4B**). The cumulative loss in SOC due to urban area was already 25,000 Mg in 1972, and increased to 86,000 Mg in 2011, reaching 141,000 Mg in 2017. The rate of annual SOC loss has increased dramatically since 2011. In the urbanisation period 1972-1984, the annual loss was 871 Mg C yr^{-1} while during the period 2011-2017, the annual loss increased to 9236 Mg C yr^{-1}.

<Fig. 4>

3.4 Change in agricultural area, 1972 - 2017

The agriculture areas in the Nile delta consist of two types of cultivated land, the old and new. The old cultivated land within the delta (see Fig 3) has an area 17,818 km^2 and this area declined to 16,083 km^2 in 2017 due to urban expansion. Since 1984 however, there has been an increase in new cultivated areas, primarily on the less fertile sandy soils of the desert area to the west of the delta (**Fig. 2**). The area of new agricultural land increased dramatically from 1984 to 1992, but the rate of increase slowed after 2003. The increase in new agricultural land, totalling 8,000 km^2 in 2017, has more than offset the loss of fertile old agricultural land to urban expansion. However, it has achieved this by expanding into previously desert areas on poor soils. Note that the increase in water bodies is largely due to an expansion of fish-farming in the more saline soil areas at the northern end of the delta closest to the Mediterranean.

3.5 Impacts on water use and fertiliser use

Water allocation for governorates in the Nile delta is largely dictated by agricultural water requirements. The directorates that receive the greatest amount of water are Beheira, Dakahlia, Sharqia and Kafr El Sheikh with 4.43, 4.38, 4.04 and 3.63 billion m^3 per year respectively (**Fig. 5**). In the study area, the water use for winter, summer, nili crops and fruits are 11.9, 23.2, 1.3, and 2.2 billion m^3 respectively (CAMPAS, 2017). Therefore, summer crops account for the greatest water use, and they are the main crops grown in the new agricultural areas on the poorer desert soils. The new cultivated land requires much more fertilisers input compared with the old cultivated land (FAO,

2005). The rate of mineral fertiliser use has increased substantially over the period 1972 – 2002 (**Fig. S6**) (www.fao.org/faostat, 2019).

<Fig. 5>

3.6 Potential for improving suitability of agricultural soils

The scenarios assessed the potential for improving the suitability of agricultural soils (with a focus on the old cultivated soils within the delta) which currently experience constraints including salinization. This was done to evaluate whether productivity of the older more fertile soils could be increased, thereby reducing the need to use poorer soils outside of the delta. The land capability classes under the current situation and improved scenario are illustrated in **Fig. 6**. Under the reference scenario of current soil conditions, the dominant land classification for both the new and old cultivated land is 'good', while the 'marginal' class was principally allocated to the *Typic Aquisalids* and *Aquic Torrifluvents* soil types located in the northern parts of the study area, and also for the sand dunes and hill-land areas in the south. In the scenario where soil salinity was decreased and drainage improved through the proposed management measures, the major land capability class in old cultivated land (*Vertic Torrifluvents*) changed to 'optimum'. The area under this class increased from 3.9% to 41.8% (**Table S8**). This indicates that although the old cultivated lands are highly fertile, there still remain some constraints of salinity which are restricting their potential for agricultural production. However, for the new cultivated areas, the main classification did not change substantially from 'good' under the improvement scenario. The total area under this class reflects a conversion of some 'moderate' land up to 'good' as well as the shift from 'good' to 'optimum' for the old cultivated areas as noted above. Management measures do not improve the soil type *Typic Aquisalids* which retained a 'marginal' classification as a result of high salinity (>16 dS/m). However, a small area has improved in *Aquic Torrifluvents*. In the remaining 'marginal' areas, the agricultural constraints are primarily restricted soil depth and water availability.

<Fig. 6>

4 Discussion

The conversion of capable agricultural land to urban use affects negatively sustainable agriculture, soil carbon storage, environment and city life (Jiang et al., 2007; Zhang et al., 2007; Seto et al., 2012; Dupras et al., 2016). Many lower and middle income countries are undergoing extremely rapid urbanisation, and our findings are consistent with studies in other countries, particularly in China where urban expansion has caused considerable loss of fertile agricultural soils, and associated environmental problems in some regions (Li et al., 2014). One reason for the rapid expansion in urban

401 area within the Nile delta in the latter part of this period, despite population growth remaining steady,
402 is linked to deregulation of planning after the Arab Spring (Grinin and Korotayev, 2019). This illustrates
403 the large influence that political and governance structures can have on land use change (Sowers and
404 Rutherford, 2018).

405 Since the soils of the Nile delta are so fertile, and have been used for agricultural production for
406 thousands of years (Mohsen et al., 2016), the two principal concerns are loss of agricultural production
407 and, from an ecosystem services perspective, the loss of soil carbon.

408 Although fertile, the delta soils contain moderate carbon contents, with carbon densities averaging
409 around 0.0133 g C cm^{-3}. However, in contrast to other soils, the carbon density is maintained down to
410 our measured depth of 75 cm, giving them a relatively high carbon stock compared with other silty
411 soils and much higher than other sandy soils (e.g. John et al., 2005; Beaumont et al., 2014; Muñoz-
412 Rojas et al., 2015, 2017). This study only assessed soil C stocks, and did not assess above-ground
413 carbon stocks. However, other studies have evaluated the impact of urban sprawl and the consequent
414 loss of dry organic matter accumulated above-ground in vegetation (Buyantuyev and Wu, 2009; Wu
415 et al., 2014; Tian and Qiao, 2014; Yan et al., 2018). This study makes the assumption that soil sealing
416 due to urban expansion results in a complete loss of carbon. It is probably the case that much carbon
417 is mineralised and therefore lost through the decomposition of organic matter as a result of
418 disturbance during construction of urban infrastructure. However, recent studies have shown that soil
419 below built areas in European cities can still retain some carbon, although typically at concentrations
420 similar to those in arable soils (Edmondson et al., 2012). In addition, the disturbance in the immediate
421 vicinity of urban areas leads to further degradation of land that is not sealed, but nonetheless becomes
422 less useful for agriculture, and less able to carry out the natural functions provided by soils (Zhao et
423 al., 2007). Although not assessed in this study, soil sealing by urbanisation affects a much broader
424 range of ecosystem services provided by soils, and not just soil carbon (Breuste et al., 2013; Dominati
425 et al., 2010; Pouyat et al., 2010).

426 Urbanization has been characterized as the most important anthropic influence on both climate and
427 land use (Kalnay and Cai, 2003; Vargo et al., 2013). Soil sealing under cities has led to increased air
428 temperatures and modified local climate (heat island effects) (Scalenghe et al., 2009; Gaur et al.,
429 2018). Meanwhile, increased or inappropriate use of pesticides and fertilizers in the remaining
430 cultivated land in the Nile delta can cause deterioration of groundwater quality (Taha et al., 2004).

431 Rapid and unplanned urban growth also causes social problems. It is often associated with poverty
432 and low environmental sustainability, and places human health at risk (Moore, 2003). Rapid

433 urbanization in South-Asian countries has led to “fringe populations”, where a significant proportion
434 of the population lives below the poverty line (Trivedi et al., 2008).

435 In Egypt, the loss of agricultural land has important consequences for agricultural production
436 (Mohamed et al., 2019). The main impact is a need to increase the area of agricultural production to
437 compensate for loss due to urbanisation. However, urbanisation may not be the only driver for the
438 expansion of agriculture outside of the delta. It may also be influenced by a number of factors,
439 including land tenure issues, small field sizes and even the infrastructure which has made agriculture
440 possible in this desert region for many thousands of years: the network of irrigation canals. Together,
441 these factors may be inhibiting the use of large-scale mechanised agriculture on the older delta soils.
442 The net result however is an expansion of intensive agriculture into the desert region to the west of
443 the delta, maintained by high inputs of fertiliser and irrigation which relies heavily on abstracted
444 groundwater. Although the delta agriculture is heavily reliant on irrigation from the Nile (CAPMAS,
445 2015), the move to use of groundwater is far less sustainable (Ahmad, 2000). The implications for
446 water availability for domestic urban populations and for future agricultural use, both from the
447 increase in agricultural area and the unsustainable use of groundwater are long-reaching.

448 The assessment of agricultural potential suggests that soil fertility could be improved through
449 management of the existing soil resource, without the need to expand the area under agriculture.
450 However, some of the measures proposed (flushing with water to desalinise soils) may also have
451 environmental costs, or put further pressure on limited water resources. An alternative may be to
452 move to crops with a lower water demand, and crops which are tolerant to salinity. These findings are
453 consistent with Tilman et al. (2002) and Manik et al. (2019) where the appropriate agriculture
454 management practices help to improve soil quality and land capability, through enhanced
455 agroecological and economical flexibility by minimizing the need for additional cultivated land. Also,
456 Setter et al. (1990) and Manik et al. (2019) indicate that improving soil drainage assist to reduce the
457 impact of waterlogging and increasing agriculture productivity. Therefore, improved soil drainage
458 enhances the availability of nutrients and water to plants, and additionally can reduce surface runoff
459 and increase infiltration (Amare et al., 2013; Vanuytrecht et al., 2014; Schmidt and Zemadim, 2015).
460 In the same context, reducing soil salinity of the salt-affected soils assist to increase crop production
461 and agriculture suitability (Horneck et al., 2007; and Zörb et al., 2019). Moreover, Wani et al. (2003)
462 reported that improvement of agriculture management in Vertisols under semiarid climates leads to
463 increased agriculture productivity and soil carbon sequestration. While this study has characterised in
464 detail the land use changes in the Nile delta, and consequences for agricultural sustainability, there
465 are a number of potential limitations. These include knowledge gaps for soil carbon in this area.
466 Although the dataset we collated is reasonably extensive, some soil types were under-represented.

Additional sampling to further improve soil carbon stock assessment in the delta should be undertaken. Two areas where there is limited understanding include sampling to assess carbon stock at depths below 75 cm, since some delta sediments are likely to be very deep, and sampling the buried soil beneath sealed surfaces to see how much carbon remains after urbanisation. This study has focused on soil carbon and agricultural suitability, however, further work could broaden this assessment to look at the impact of urbanisation on a wider range of ecosystem services provided by the Nile delta region.

5 Conclusions

Over the last four decades (1972-2017), there has been considerable loss of fertile agricultural land that has high carbon stocks, with consequences for loss agricultural production. Over the same period, there has been a spread of agriculture into desert land to the west. However, the agricultural production methods are less sustainable, based on high levels of water use from the river Nile and groundwater abstraction and high agro-chemical use.

The continued loss of the highly fertile cultivated land due to rapid urban sprawl represents a substantial threat to agriculture land sustainability and Egyptian food security.

This paper has shown an integrated assessment of the effects of urban sprawl, making use of a wide set of techniques, including remote sensing, GIS, ecosystem service models (InVEST) and agriculture models (MicroLEIS) underpinned by primary data collection on soil properties. This approach has helped to guide recommendations for more sustainable future options for conserving the limited agricultural land by improving agriculture management practices to increase agriculture production, and reducing expected harmful environmental impacts due to urbanisation.

6 Acknowledgments

We thank the British Council (Newton Fund, UK) and Science and Technology Development Fund (STDF, Egypt) for funding this project (ID 27663). We also thank the Talented Young Scientist Program (TYSP), China Science and Technology Exchange Center, for its support.

7 References

Abd El-Kawy, O. R., Rød, J. K., Ismail, H. A., Suliman, A. S., 2011. Land use and land cover change detection in the western Nile delta of Egypt using remote sensing data. Appl. Geogr. 31, 483-494. doi.org/10.1016/j.apgeog.2010.10.012

Abdel-Dayem, S., Ritzema, H. P., 1990. Verification of drainage design criteria in the Nile Delta, Egypt. Irrig. Drain. Sys. 4(2), 117-131. doi.org/10.1007/BF01102801

Abd-Elmabod, S.K., Bakr, N., Muñoz-Rojas, M., Pereira, P., Zhang, Z., Cerdà, A., Jordán, A., Mansour, H., De la Rosa, D., Jones, L. 2019. Assessment of Soil Suitability for Improvement of Soil Factors and Agricultural Management. Sustainability. 11, 1588. doi.org/10.3390/su11061588

Abd-Elmabod, S.K.; Jordán, A.; Fleskens, L.; Phillips, J.D.; Muñoz-Rojas, M.; Van der Ploeg, M.; Anaya-Romero, M.; De la Rosa, D. 2017. Modelling agricultural suitability along soil transects under current conditions and improved scenario of soil factors, in: Pereira, P., Brevik, E., Muñoz-Rojas, M., Miller, B (Eds.), Soil Mapping and Process Modeling for Sustainable Land Use Management; Elsevier: Amsterdam, The Netherland; 193–219; ISBN: 9780128052006.

Aboukhaled, A., Arar, A., Balba, A. M., Bishay, B. G., Kadry, L. T., Rutema, P. E., Taher, A., 1975. Research on crop water use, salt affected soils and drainage in the Arab Republic of Egypt. Food and Agriculture Organization of the United Nations, Near East Regional Office, Cairo, Egypt, 62-79.

Abrol, I. P., Yadav, J. S. P., Massoud, F. I., 1988. Salt-affected soils and their management (No. 39). Food & Agriculture Org.

Abu-hashim, M., Elsayed, M., Belal, A. E., 2016. Effect of land-use changes and site variables on surface soil organic carbon pool at Mediterranean Region. J. Afr. Earth Sci. 114, 78-84. doi:10.1016/j.jafrearsci.2015.11.020

Ahmad, M., 2000. Water pricing and markets in the near east: Policy issues and options. Water Policy. 2, 229-242. doi:10.1016/S1366-7017(99)00006-9

Ali, R.R., 2003. Evaluation of land degradation of some areas in middle and north Nile delta, Egypt. PhD thesis, Fac. Agric., Cairo Unvi. Egypt.

Amare T., Terefe A., Selassie Y. G., Yitaferu B., Wolfgramm B., Hurni H., 2013. Soil properties and crop yields along the terraces and toposequece of Anjeni Watershed, Central Highlands of Ethiopia. J. Agric. Sci. 5:134. doi: 10.5539/jas.v5n2p134

Anaya-Romero, M., Abd-Elmabod, S. K., Muñoz-Rojas, M., Castellano, G., Ceacero, C. J., Alvarez, S., S., Méndez, M., De la Rosa, D., 2015. Evaluating soil threats under climate change scenarios in the Andalusia region, southern Spain. Land Degrad Dev. 26(5), 441-449. doi:10.1002/ldr.2363

527 ASRT., 2009. Preparation of Land Data Base for Agriculture Use" fifth report. Academy of Scientific
528 research and technology (ASRT), Cairo, Egypt.

529 Bai, X., Dawson, R. J., Ürge-Vorsatz, D., Delgado, G. C., Salisu Barau, A., Dhakal, S., Dodman, D.,
530 Leonardsen, L., Masson-Delmotte, V., Roberts, D., Schultz, S., 2018. Six research priorities for cities
531 and climate change. Nature. 555(7694), 23-25. doi:10.1038/d41586-018-02409-z

532 Ball, J., 1939. Contribution to the Geology of Egypt. Egyptian Government Press.

533 Beaumont N.J., Jones, L., Garbutt, A., Hansom, J.D., Toberman, M., 2014. The value of carbon
534 sequestration and storage in UK coastal habitats. Estuarine, Coast. Shelf Sci. 137, 32-40.
535 doi.org/10.1016/j.ecss.2013.11.022

536 Breuste, J., Haase, D. Elmqvist, T., 2013. Urban landscapes and ecosystem services. Ecosyst. Serv. Agri.
537 Urban Landscapes, 83-104. doi.org/10.1002/9781118506271.ch6

538 Bugnot, A. B., Hose, G. C., Walsh, C. J., Floerl, O., French, K., Dafforn, K. A., . . . Hahs, A. K., 2019. Urban
539 impacts across realms: Making the case for inter-realm monitoring and management. Sci. Total
540 Environ. 648, 711-719. doi:10.1016/j.scitotenv.2018.08.134

541 Buyantuyev, A., Wu, J., 2009. Urbanization alters spatiotemporal patterns of ecosystem primary
542 production: A case study of the phoenix metropolitan region, USA. J. Arid Environ. 73, 512-520.
543 doi:10.1016/j.jaridenv.2008.12.015

544 Campbell, J. B., Wynne, R. H. ,2011. Introduction to remote sensing. Guilford Press.

545 CAPMAS. 2015. Statistical Year Book" Central Agency for Public Mobilization and Statistics (CAPMAS),
546 annual report 2015, Cairo, Egypt. http://www.capmas.gov.eg

547 CAPMAS., 2017. "Statistical Year Book" Central Agency for Public Mobilization and Statistics (CAPMAS),
548 annual report 2017, Cairo, Egypt. http://www.capmas.gov.eg

549 Carlson, T. N., Traci Arthur, S., 2000. The impact of land use - land cover changes due to urbanization on
550 surface microclimate and hydrology: A satellite perspective. Global Planet. Change. 25, 49-65.
551 doi:10.1016/S0921-8181(00)00021-7

552 CLAC., 2016. The Climatic Stations of Nile delta. Annual report. Central Laboratory for Agricultural
553 Climate (CLAC). Cairo, Egypt.

554 Concepción, E. D., Moretti, M., Altermatt, F., Nobis, M. P., Obrist, M. K., 2015. Impacts of urbanisation
555 on biodiversity: The role of species mobility, degree of specialisation and spatial scale. Oikos. 124,
556 1571-1582. doi:10.1111/oik.02166

557 Crist, P. J., Kohley, T. W., Oakleaf, J., 2000. Assessing land-use impacts on biodiversity using an expert
558 systems tool. Landscape Ecol. 15, 47-62. doi:10.1023/A:1008117427864

559 Cui, X., Fang, C., Liu, H., Liu, X., 2019. Assessing sustainability of urbanization by a coordinated
560 development index for an urbanization-resources-environment complex system: A case study of
561 Jing-Jin-Ji region, china. Ecol. Indic. 96, 383-391. doi:10.1016/j.ecolind.2018.09.009

562 De Kimpe, C.R. and Morel, J.L., 2000. Urban soil management: a growing concern. Soil Sci. 165, 31-40.
563 doi : 10.1097/00010694-200001000-00005

564 De la Rosa, D. and D. Magaldi. 1982. Rasgos metodológicos de un sistema de evaluación de tierras para
565 regiones Mediterráneas. Soc. Esp. Cien. Suelo. Madrid.

566 De la Rosa, D., Anaya-Romero, M., Diaz-Pereira, E., Heredia, N., Shahbazi, F., 2009. Soil-specific agro-
567 ecological strategies for sustainable land use - A case study by using MicroLEIS DSS in Sevilla province
568 (Spain). Land use Policy. 26, 1055-1065. doi:10.1016/j.landusepol.2009.01.004

569 De La Rosa, D., Cardona, F., Almorza, J., 1981. Crop yield predictions based on properties of soils in
570 Sevilla, Spain. Geoderma. 25, 267-274. doi:10.1016/0016-7061(81)90040-9

571 De La Rosa, D., Mayol, F., Diaz-Pereira, E., Fernandez, M., De La Rosa Jr., D., 2004. A land evaluation
572 decision support system (MicroLEIS DSS) for agricultural soil protection: With special reference to
573 the mediterranean region. Environ. Modell. Softw. 19, 929-942. doi:10.1016/j.envsoft.2003.10.006

574 De la Rosa, D., Moreno, J. A., Garcia, L. V., Almorza, J.,1992. MicroLEIS: A microcomputer-based
575 mediterranean land evaluation information system. Soil Use Manage. 8, 89-96. doi:10.1111/j.1475-
576 2743.1992.tb00900.x

577 Demirel, H., Ozcinar, C., Anbarjafari, G., 2010. Satellite image contrast enhancement using discrete
578 wavelet transform and singular value decomposition. IEEE GRSL. 7, 333-337.
579 10.1109/LGRS.2009.2034873

580 Deng, X., Huang, J., Rozelle, S., Uchida, E., 2006. Cultivated land conversion and potential agricultural
581 productivity in china. Land use Policy. 23, 372-384. doi:10.1016/j.landusepol.2005.07.003

582 Dewidar, K. M., 2004. Detection of land use/land cover changes for the northern part of the Nile Delta
583 (burullus region), Egypt. Int. J Remote Sens., 25, 4079-4089. doi:10.1080/01431160410001688312

584 Dominati, E., Patterson, M., Mackay, A., 2010. A framework for classifying and quantifying the natural
585 capital and ecosystem services of soils. Ecol. Econ. 69, 1858-1868.
586 doi:10.1016/j.ecolecon.2010.05.002

587 Dupras, J., Marull, J., Parcerisas, L., Coll, F., Gonzalez, A., Girard, M., Tello, E., 2016. The impacts of
588 urban sprawl on ecological connectivity in the Montreal Metropolitan Region. Environ. Sci. Policy.
589 58, 61-73. doi.org/10.1016/j.envsci.2016.01.005

590 Edmondson, J. L., Davies, Z. G., McHugh, N., Gaston, K. J., Leake, J. R., 2012. Organic carbon hidden in
591 urban ecosystems. Sci. Rep. 2 doi:10.1038/srep00963

592 Ezzeldin, M. M., El-Alfy, K. S., Abdel-Gawad, H. A., Abd-Elmaboud, M. E., 2016. Land use changes in the
593 Eastern Nile Delta Region; Egypt using multi-temporal remote sensing techniques. Int. J. Sci. Eng.
594 Res. 7(12), 78-98.

595 Fernandes, K., 2002. Urban development and new towns in the Third World, lessons from the new
596 Bombay experience. Habitat Int. 26, 134–135.

597 Food and Agriculture Organization of the United Nations (FAO-UN). 2005. Fertilizer use by crop in Egypt.
598 Rome, Italy

599 Gandhi, G. M., Parthiban, S., Thummalu, N., Christy, A., 2015. NDVI: Vegetation change detection using
600 remote sensing and GIS - A case study of Vellore district. Procedia Comput. Sci. 571199-1210.
601 doi:10.1016/j.procs.2015.07.415

602 García-Nieto, A. P., Geijzendorffer, I. R., Baró, F., Roche, P. K., Bondeau, A., Cramer, W., 2018. Impacts
603 of urbanization around Mediterranean cities: Changes in ecosystem service supply. Ecol. Indic. 91,
604 589-606. doi:10.1016/j.ecolind.2018.03.082

605 Gaur, A., Eichenbaum, M. K., Simonovic, S. P., 2018. Analysis and modelling of surface Urban Heat Island
606 in 20 Canadian cities under climate and land-cover change. J. Environ. Manage. 206, 145-157.
607 doi.org/10.1016/j.jenvman.2017.10.002

608 GeoSpatial Analysis 5th Edition, 2018 Smith M. J., Goodchild, M. F., Longley, P. A.
609 http://www.spatialanalysisonline.com/HTML/?profiles_and_curvature.htm

610 Gomes, E., Banos, A., Abrantes, P., Rocha, J., Kristensen, S. B. P., Busck, A., 2019. Agricultural land
611 fragmentation analysis in a peri-urban context: From the past into the future. Ecol. Indic. 97, 380-
612 388. doi:10.1016/j.ecolind.2018.10.025

613 Grădinaru, S. R., Kienast, F., Psomas, A., 2019. Using multi-seasonal landsat imagery for rapid
614 identification of abandoned land in areas affected by urban sprawl. Ecol. Indic. 96, 79-86.
615 doi:10.1016/j.ecolind.2017.06.022

616 Haase, D., Nuissl, H., 2007. Does urban sprawl drive changes in the water balance and policy?. the case
617 of leipzig (germany) 1870-2003. Landscape Urban Plan. 8, 1-13.
618 doi:10.1016/j.landurbplan.2006.03.011

619 Han, J., Huang, Y., Zhang, H., Wu, X., 2019. Characterization of elevation and land cover dependent
620 trends of NDVI variations in the Hexi region, northwest china. J. Environ. Manage. 232, 1037-1048.
621 doi:10.1016/j.jenvman.2018.11.069

622 He, C., Zhang, D., Huang, Q. and Zhao, Y., 2016. Assessing the potential impacts of urban expansion on
623 regional carbon storage by linking the LUSD-urban and InVEST models. Environ. Modell. Softw. 75,
624 44-58. doi.org/10.1016/j.envsoft.2015.09.015

625 Hegazy, I. R., Kaloop, M. R., 2015. Monitoring urban growth and land use change detection with GIS and
626 remote sensing techniques in Daqahlia governorate Egypt. Intern. J. Sust. Built Environ. 4, 117-124.
627 doi:10.1016/j.ijsbe.2015.02.005

628 Horneck, D. A., Ellsworth, J. W., Hopkins, B. G., Sullivan, D. M., and Stevens, R. G., 2007. Managing salt-
629 affected soils for crop production, Oregon State University, University of Idho Washington State
630 University, A Pacific Northwest Extension Publication, PNW 601-E.

631 Islam, K. R., Weil, R. R., 2000. Land use effects on soil quality in a tropical forest ecosystem of
632 bangladesh. Agriculture, Ecosyst. Environ. 79, 9-16. doi:10.1016/S0167-8809(99)00145-0

633 ITT., 2009. ITT corporation ENVI 4.7 software, 1133 Westchester Avenue, White Plains, NY 10604, USA.

634 Jiang, F., Liu, S., Yuan, H., Zhang, Q., 2007. Measuring urban sprawl in Beijing with geo-spatial indices. J.
635 Geogr. Sci. 17(4), 469-478. doi.org/10.1007/s11442-007-0469-z

636 John, B., Yamashita, T., Ludwig, B., Flessa, H. 2005. Storage of organic carbon in aggregate and density
637 fractions of silty soils under different types of land use. Geoderma. 128, 63-79.
638 doi:10.1016/j.geoderma.2004.12.013

639 Kalnay, E., Cai, M., 2003. Impact of urbanization and land-use change on climate. Nature. 423(6939),
640 528-531. doi: 10.1038/nature01675

641 Kassim, Y., Mahmoud, M., Kurdi, S., Breisinger, C. 2018. An agricultural policy review of Egypt: First
642 steps towards a new strategy (Vol. 11). Intl Food Policy Res Inst.

643 Kotb, T. H., Watanabe, T., Ogino, Y., Tanji, K. K., 2000. Soil salinization in the Nile Delta and related
644 policy issues in Egypt. Agr. Water Manage.43(2), 239-261. doi.org/10.1016/S0378-3774(99)00052-9

645 Lavy, B.L., Julian, J.P. and Jawarneh, R.N., 2016. The Impact of Past and Future Urban Expansion on Soil
646 Resources in Central Arkansas, 1994–2030. Pap. Appl. Geogr. 2(1),25-39.
647 doi.org/10.1080/23754931.2015.1106972

648 Leeson, G. W., 2018. The Growth, Ageing and Urbanisation of our World. Journal of Population Ageing,
649 1-9. doi.org/10.1007/s12062-018-9225-7

650 Li, C., Zhao, J., Thinh, N. and Xi, Y., 2018. Assessment of the effects of urban expansion on terrestrial
651 carbon storage: A case study in Xuzhou City, China. Sustainability. 10(3), 647. doi:
652 10.3390/su10030647

653 Li, X. Y., Li, H., Liu, H. J., 2014. Effects of urbanization on black soil: A remote sensing perspective. Appl.
654 Mech. Mater.535, 478-482. doi.org/10.4028/www.scientific.net/AMM.535.478

655 Li, Y., Wang, G., Wang, J., Jia, Z., Zhou, Y., Wang, C., Li, Y., Zhou, S., 2019. Determination of influencing
656 factors on historical concentration variations of PAHs in West Taihu Lake, China. Environ. Pollut.,
657 249, 573-580. doi.org/10.1016/j.envpol.2019.03.055

658 Lillesand, T.M., R.W. Kiefer., 2007. Remote sensing and image interpretation. 5th edition. New York,
659 John Wiley and Sons.

660 Liu, Y., Lü, Y., Fu, B., Harris, P., Wu, L. 2019. Quantifying the spatio-temporal drivers of planned
661 vegetation restoration on ecosystem services at a regional scale. Sci. Total Environ. 650, 1029-1040.
662 doi:10.1016/j.scitotenv.2018.09.082

663 Liu, Y., Song, W., Deng, X. 2019. Understanding the spatiotemporal variation of urban land expansion in
664 oasis cities by integrating remote sensing and multi-dimensional DPSIR-based indicators. Ecol. Indic.
665 96, 23-37. doi:10.1016/j.ecolind.2018.01.029

666 Long, H., Ge, D., Zhang, Y., Tu, S., Qu, Y., Ma, L., 2018. Changing man-land interrelations in China's
667 farming area under urbanization and its implications for food security. J. Environ. Manage. 209, 440-
668 451. doi.org/10.1016/j.jenvman.2017.12.047

669 Maas, E. V., Grattan, S. R., 1999. Crop yields as affected by salinity. Agronomy. 38, 55-110. doi:
670 10.2134/agronmonogr38.c3

671 Manik, S. N., Pengilley, G., Dean, G., Field, B., Shabala, S., Zhou, M., 2019. Soil and Crop Management
672 Practices to Minimize the Impact of Waterlogging on Crop Productivity. Front. Plant Sci. 10. doi:
673 10.3389/fpls.2019.00140

674 McNabb, D. E., 2019. The Population Growth Barrier. In Global Pathways to Water Sustainability.
675 Palgrave Macmillan, Cham, 67-81. doi.org/10.1007/978-3-030-04085-7_5

676 Mohamed, E. S., Belal, A., Shalaby, A., 2015. Impacts of soil sealing on potential agriculture in Egypt
677 using remote sensing and GIS techniques. Eurasian Soil Sci. 48, 1159-1169.

678 Mohamed, E., Belal, A. A., Ali, R. R., Saleh, A., Hendawy, E. A., 2019. Land degradation, in: El-Ramady H.,
679 Alshaal, T., Bakr N., Elbana T., Mohamed, E., Belal, A. (Eds.), The Soils of Egypt. 159-174. Springer,
680 Cham.

681 Mohamedin, A. A. M., Awaad, M. S., Ahmed, A. R., 2010. The negative role of soil salinity and
682 waterlogging on crop productivity in the northeastern region of the Nile Delta, Egypt. Res. J. Agri.
683 Biol. Sci. 6(4), 378-385.

684 Mohsen M. E., Kassem S. E., Hossam A. A., Mahmoud E. A., 2016. Land Use Changes in the Eastern Nile
685 Delta Region; Egypt Using Multi-temporal Remote Sensing Techniques. Int. J. Scient. Eng. Res. 7, 78-
686 98.

687 Moore, M., Gould, P., Keary, B. S., 2003. Global urbanization and impact on health. Int. J. Hyg. Envir.
688 Heal. 206, 269-278.

689 Muñoz-Rojas, M.; Abd-Elmabod, S.K.; Zavala, L.M.; De la Rosa, D.; Jordán, A. 2017. Climate change
690 impacts on soil organic carbon stocks of Mediterranean agricultural areas: A case study in Northern
691 Egypt. Agric. Ecosyst. Environ. 238, 142–152. doi.org/10.1016/j.agee.2016.09.001

692 Muñoz-Rojas, M.; Jordán. A.; Zavala, L.M.; De la Rosa, D.; Abd-Elmabod, S.K.; Anaya-Romero, M. 2015.
693 Impact of land use and land cover changes on organic carbon stocks in Mediterranean soils (1956–
694 2007). Land Degrad. Dev. 26, 168–179. doi.org/10.1002/ldr.2194

695 Nageswara Rao, P. P., Shobha, S. V., Ramesh, K. S., Somashekhar, R. K., 2005. Satellite-based
696 assessment of agricultural drought in Karnataka state. J Indian Soc. Remote. 33, 429-434.
697 doi:10.1007/BF02990014

698 Nelson, E., Mendoza, G., Regetz, J., Polasky, S., Tallis, H., Cameron, D. R., . . . Shaw, M. R., 2009.
699 Modeling multiple ecosystem services, biodiversity conservation, commodity production, and
700 tradeoffs at landscape scales. Front. Ecol. Environ. 7, 4-11. doi:10.1890/080023

701 Nizeyimana, E. L., Petersen, G. W., Imhoff, M. L., Sinclair, H. R., Waltman, S. W., Reed-Margetan, D. S., ...
702 & Russo, J. M. (2001). Assessing the impact of land conversion to urban use on soils with different
703 productivity levels in the USA. Soil Sci. Soc. Am. J. 65, 391-402.

704 Osama, S., Elkholy, M., Kansoh, R. M., 2017. Optimization of the cropping pattern in Egypt. Alex. Eng. J.
705 56, 557-566. doi:10.1016/j.aej.2017.04.015

706 Park, T., Ganguly, S., TØmmervik, H., Euskirchen, E. S., HØgda, K. -., Karlsen, S. R., . . . Myneni, R. B.,
707 2016. Changes in growing season duration and productivity of northern vegetation inferred from
708 long-term remote sensing data. Environ. Res Lett., 11. doi:10.1088/1748-9326/11/8/084001

709 Pouyat, R.V., Szlavecz, K., Yesilonis, I.D., Groffman, P.M. and Schwarz, K., 2010. Chemical, physical, and
710 biological characteristics of urban soils. Urban Ecosyst. Ecol. 119-152.

711 Rafferty, J. P. 2019. Urban Sprawl. Encyclopedia Britannica. https://www.britannica.com/topic/urban-
712 sprawl.

713 Redhead, J. W., Stratford, C., Sharps, K., Jones, L., Ziv, G., Clarke, D., Oliver, T.H., Bullock, J. M., 2016.
714 Empirical validation of the InVEST water yield ecosystem service model at a national scale. Sci. Total
715 Environ. 569-570, 1418-1426. doi:10.1016/j.scitotenv.2016.06.227

716 Rizvi, S., Pagnutti, C., Fraser, E., Bauch, C. T., Anand, M.,2018. Correction: Global land use implications of
717 dietary trends. PLoS ONE. 13(10) doi:10.1371/journal.pone.0205312

718 Scalenghe, R., Marsan, F. A. 2009. The anthropogenic sealing of soils in urban areas. Landscape Urban
719 Plan. 90, 1-10. doi.org/10.1016/j.landurbplan.2008.10.011

720 Schmidt E., Zemadim B. 2015. Expanding sustainable land management in Ethiopia: scenarios for
721 improved agricultural water management in the Blue Nile. Agric. Water Manag. 158 166–178.
722 10.1016/j.agwat.2015.05.001.

723 Seto, K. C., Güneralp, B., Hutyra, L. R., 2012. Global forecasts of urban expansion to 2030 and direct
724 impacts on biodiversity and carbon pools. P. Natl. A. Sci., 109(40), 16083-16088.
725 doi.org/10.1073/pnas.1211658109

726 Setter T., Belford B.,1990. Waterlogging: how it reduces plant growth and how plants can overcome its
727 effects. J. Dep. Agric. West. Aust. Ser. 4 51–55

728 Shalaby, A. A., Ali, R. R., Gad, A., 2012. Urban sprawl impact assessment on the agricultural land in Egypt
729 using remote sensing and GIS: A case study, Qalubiya Governorate. Journal of land use science, 7(3),
730 261-273. doi.org/10.1080/1747423X.2011.562928

731 Shalaby, A., 2012. Assessment of Urban Sprawl Impact on the Agricultural Land in the Nile Delta of
732 Egypt Using Remote Sensing and Digital Soil Map. Int. J. of Environ. and Sci.1(4), 253-262.

733 Shalaby, A., Moghanm, F. S., 2015. Assessment of urban sprawl on agricultural soil of northern Nile
734 Delta of Egypt using RS and GIS. Chinese Geogr. Sci., 25, 274-282. doi:10.1007/s11769-015-0748-z

735 Shalaby, A., Tateishi, R., 2007. Remote sensing and GIS for mapping and monitoring land cover and
736 land-use changes in the northwestern coastal zone of Egypt. Appl. Geogr. 27, 28-41.
737 doi:10.1016/j.apgeog.2006.09.004

738 Sharps, K., Masante, D., Thomas, A., Jackson, B., Cosby, B., Emmett, B., Jones, L., 2017. Comparing
739 strengths and weaknesses of three ecosystem services modelling tools in a diverse UK river
740 catchment. Sci. Total Environ., 584-585, 118-130. doi:10.1016/j.scitotenv.2016.12.160

741 Shastri, H., Ghosh, S., 2019. Urbanisation and Surface Urban Heat Island Intensity (SUHII). Climate
742 Change Signals and Response, 73-90. doi.org/10.1007/978-981-13-0280-0_5

743 Sowers, J. L., Rutherford, B. K., 2018. Revolution and Counterrevolution in Egypt. In The Arab Spring, 40-
744 71. Routledge.

745 Sudmeier-Rieux, K., Fra.Paleo, U., Garschagen, M., Estrella, M., Renaud, F. G., Jaboyedoff, M., 2015.
746 Opportunities, incentives and challenges to risk sensitive land use planning: Lessons from nepal,
747 spain and vietnam. Int. J. Disast. Risk Re., 14, 205-224. doi:10.1016/j.ijdrr.2014.09.009

748 Suliman, M. K., 1991. Universities and Development of the Desert land in the ARE. The second annual
749 University conference, Cairo, 2-5 November, Egypt.

750 Sultan, M., Fiske, M., Stein, T., Gamal, M., Hady, Y.A., El Araby, H., Madani, A., Mehanee, S. and Becker,
751 R., 1999. Monitoring the urbanization of the Nile Delta, Egypt. Ambio, 28(7), pp.628-631.

752 Taha, A. A., El-Mahmoudi, A. S., El-Haddad, I. M., 2004. Pollution sources and related environmental
753 impacts in the new communities southeast Nile Delta, Egypt. Emirates J. Engin. Res. 9, 35-49.

754 Tang, J., Di, L., 2019. Past and Future Trajectories of Farmland Loss Due to Rapid Urbanization Using
755 Landsat Imagery and the Markov-CA Model: A Case Study of Delhi, India. Remote Sens., 11, 180.
756 doi.org/10.3390/rs11020180

757 Tian, G., Qiao, Z., 2014. Assessing the impact of the urbanization process on net primary productivity in
758 china in 1989-2000. Environ. Pollut., 184, 320-326. doi:10.1016/j.envpol.2013.09.012

759 Tilman, D., Cassman K.G., Matson, P. A., Naylor, R., Polasky, S., 2002. Agricultural sustainability and
760 intensive production practices. Nature. 418(6898), 671-7. doi: 10.1038/nature01014

761 Trivedi, J. K., Sareen, H., Dhyani, M., 2008. Rapid urbanization-Its impact on mental health: A South
762 Asian perspective. Indian J. Psychiat. 50, 161. doi: 10.4103/0019-5545.43623

763 Umesha, S., Manukumar, H. M., Chandrasekhar, B.,2018. Sustainable Agriculture and Food Security.
764 Biotechnology for Sustainable Agriculture (67-92). Woodhead Publishing.

765 United Nations Human Settlements Programme (UN-Habitat), 2016. Urbanization and development:
766 emerging futures, world cities report 2016. Nairobi.

767 United Nations Population Division (UNPD), 2018. World Urbanization Prospects: 2018 Revision.
768 [Online, accessed 14th July 2019] https://data.worldbank.org/indicator/sp.urb.totl.in.zs

769 Vanuytrecht, E., Raes, D., Steduto, P., Hsiao, T. C., Fereres, E., Heng, L. K., ..., Moreno, P. M., 2014.
770 AquaCrop: FAO's crop water productivity and yield response model. Environ. Modell. Softw., 62,
771 351-360. doi.org/10.1016/j.envsoft.2014.08.005

772 Vargo, J., Habeeb, D., Stone Jr, B., 2013. The importance of land cover change across urban–rural
773 typologies for climate modeling. J. Environ. Manage. 243-252.
774 doi.org/10.1016/j.jenvman.2012.10.007

775 Vasenev, V.I., Stoorvogel, J.J., Leemans, R., Valentini, R. and Hajiaghayeva, R.A., 2018. Projection of
776 urban expansion and related changes in soil carbon stocks in the Moscow Region. J. Clean. Prod. 170,
777 902-914. doi.org/10.1016/j.jclepro.2017.09.161

778 Wang, J., Zhou, W., Pickett, S. T., Yu, W., Li, W., 2019. A multiscale analysis of urbanization effects on
779 ecosystem services supply in an urban megaregion. Sci. Total Environ. 662, 824-833.
780 doi.org/10.1016/j.scitotenv.2019.01.260

781 Wang, K., Li, T., Wei, J. 2019. Exploring Drought Conditions in the Three River Headwaters Region from
782 2002 to 2011 Using Multiple Drought Indices. Water, 11, 190. doi.org/10.3390/w11020190

783 Wani, S. P., Pathak, P., Jangawad, L. S., Eswaran, H., Singh, P., 2003. Improved management of Vertisols
784 in the semiarid tropics for increased productivity and soil carbon sequestration. Soil Use Manage.,
785 19(3), 217-222. doi.org/10.1111/j.1475-2743.2003.tb00307.x

786 Weber, A., Fohrer, N., Möller, D. 2001. Long-term land use changes in a mesoscale watershed due to
787 socio-economic factors - effects on landscape structures and functions. Ecol. Model., 140, 125-140.
788 doi:10.1016/S0304-3800(01)00261-7

789 Weber, C., Puissant, A., 2003. Urbanization pressure and modeling of urban growth: Example of the
790 tunis metropolitan area. Remote Sens. Environ., 86, 341-352. doi:10.1016/S0034-4257(03)00077-4

791 Wen, Y., Liu, X., Bai, Y., Sun, Y., Yang, J., Lin, K., ... Yan, Y., 2019. Determining the impacts of climate
792 change and urban expansion on terrestrial net primary production in China. J. Environ. Manage. 240,
793 75-83. doi.org/10.1016/j.jenvman.2019.03.071

794 Wu, S., Zhou, S., Chen, D., Wei, Z., Dai, L., Li, X., 2014. Determining the contributions of urbanisation and
795 climate change to NPP variations over the last decade in the Yangtze river delta, china. Sci. Total
796 Environ., 472, 397-406. doi:10.1016/j.scitotenv.2013.10.128

797 Yang, Y., Zhu, J., Zhao, C., Liu, S., Tong, X., 2011. The spatial continuity study of NDVI based on kriging
798 and BPNN algorithm. Math. Comput. Model., 54, 1138-1144. doi:10.1016/j.mcm.2010.11.046

799 Zhang, F., Yushanjiang, A., Jing, Y.Q., 2019. Assessing and predicting changes of the ecosystem service
800 values based on land use/cover change in Ebinur Lake Wetland National Nature Reserve, Xinjiang,
801 China. Sci. Total Environ., 656, 1133-1144. doi:10.1016/j.scitotenv.2018.11.444

802 Zhang, X., Chen, J., Tan, M., Sun, Y., 2007. Assessing the impact of urban sprawl on soil resources of
803 Nanjing city using satellite images and digital soil databases. Catena. 69(1), 16-30.
804 doi.org/10.1016/j.catena.2006.04.020

805 Zhao, Y.G., Zhang, G.L., Zepp, H. and Yang, J.L., 2007. Establishing a spatial grouping base for surface soil
806 properties along urban–rural gradient—A case study in Nanjing, China. Catena. 69, 74-81.
807 doi:10.1016/j.catena.2006.04.017

808 Zhou, Y., Guo, L., Liu, Y.,2019. Land consolidation boosting poverty alleviation in China: Theory and
809 practice. Land Use Policy. 82, 339-348. doi:10.1016/j.landusepol.2018.12.024.

810 Zörb, C., Geilfus, C. M., Dietz, K. J., 2019. Salinity and crop yield. Plant Biol. 21, 31-38.
811 doi.org/10.1111/plb.12884

812

Table 1. Changes of soil map unit areas (km^2) between 1972 and 2017. (A) difference between 1984 and 1972, (B) difference between 1992 and 1984, (C) difference between 2003 and 1992, (D) difference between 2011 and 2003, (E) difference between 2017 and 2011, (F) total difference between 2017 and 1972.

Soil map unit	Year						Changes					
	1972	**1984**	**1992**	**2003**	**2011**	**2017**	**A**	**B**	**C**	**D**	**E**	**F**
Vertic Torrifluvents	12704.9	12571.4	12517.2	12360.4	12089.6	11735.5	-133.5	-54.2	-156.8	-270.9	-354.0	-969.4
Typic Torrifluvents	2850.8	2832.9	2817.1	2795.0	2749.5	2670.7	-17.9	-15.9	-22.0	-45.6	-78.7	-180.1
Typic Quartizipsamments	5742.8	5729.2	5706.5	5675.1	5592.1	5479.7	-13.6	-22.8	-31.4	-83.1	-112.4	-263.2
Typic Torriorthents	2095.7	2090.5	2087.8	2078.5	2054.2	2013.1	-5.2	-2.6	-9.3	-24.3	-41.1	-82.6
Typic Petrogypsids	100.9	99.3	96.6	93.0	87.4	83.8	-1.6	-2.7	-3.6	-5.6	-3.7	-17.1
Typic Haplogypsids	946.1	945.4	944.8	942.6	939.7	926.2	-0.7	-0.6	-2.2	-2.9	-13.5	-19.8
Typic Aquisalids	2241.4	2233.6	2208.5	2194.7	2161.3	2122.4	-7.8	-25.2	-13.8	-33.4	-38.9	-119.0
Typic Torripsamments	2096.8	2092.7	2082.2	2072.8	2050.5	1990.5	-4.1	-10.6	-9.4	-22.3	-60.1	-106.3
Typic Haplosalids	147.2	145.8	144.8	141.8	134.4	121.5	-1.4	-0.9	-3.0	-7.4	-12.9	-25.7
Typic Haplocalcids	2211.0	2207.5	2203.9	2196.9	2165.7	2102.8	-3.5	-3.6	-7.0	-31.2	-62.9	-108.2
Aquic Torrifluvents	938.1	933.4	927.0	923.0	913.7	896.1	-4.7	-6.4	-4.0	-9.3	-17.6	-42.0
Hilland	1070.0	1068.7	1067.4	1065.2	1054.6	1042.4	-1.3	-1.3	-2.2	-10.6	-12.2	-27.6
Rock land	4811.9	4805.4	4803.7	4786.1	4747.2	4672.3	-6.5	-1.7	-17.6	-39.0	-74.9	-139.7
Water bodies	2396.0	2386.9	2382.4	2369.3	2331.8	2304.0	-9.2	-4.5	-13.1	-37.5	-27.7	-92.0
Urban	451.6	662.5	815.6	1111.0	1733.9	2644.4	210.9	153.1	295.4	622.9	910.5	2192.8
Total	**40805.3**	**40805.3**	**40805.3**	**40805.3**	**40805.3**	**40805.3**	**0.0**	**0.0**	**0.0**	**0.0**	**0.0**	**0.0**

Negative (-) sign denote a decrease in area

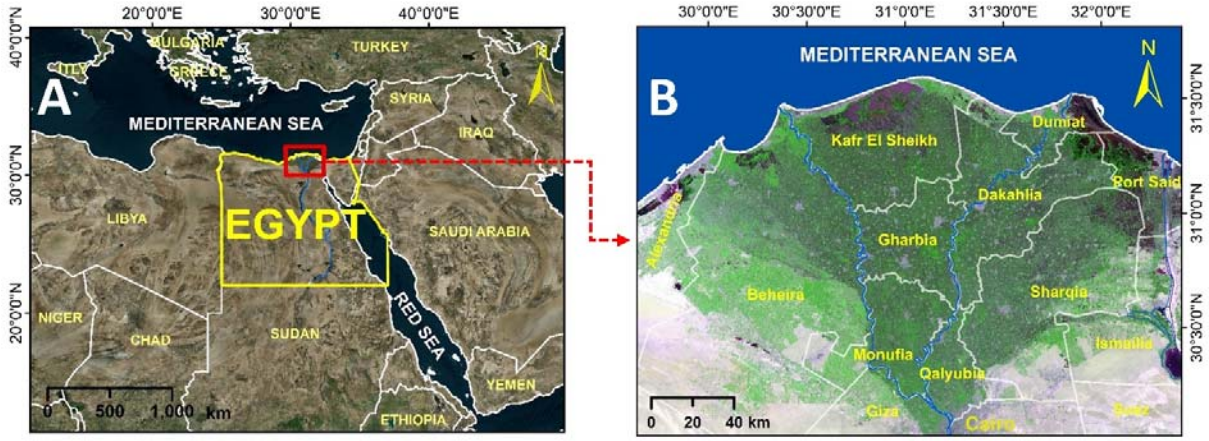

Fig. 1. Location of the study area. A, location of Egypt; B, Nile Delta and its governorates.

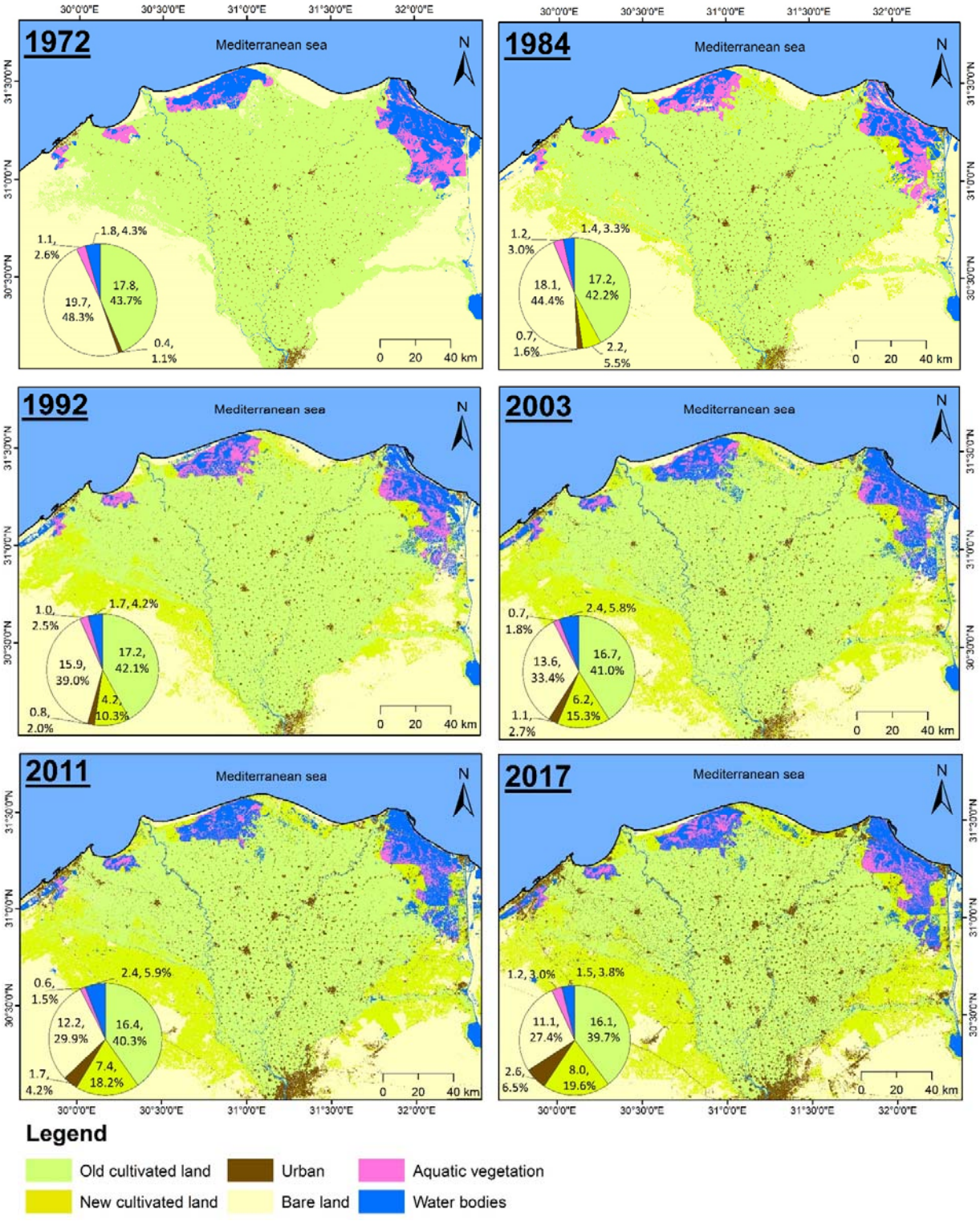

Fig. 2. Urban expansion and change in the major land cover classes from 1972-2017. The pie chart illustrates the proportion occupied by each land cover class (x1000km^2, and %).

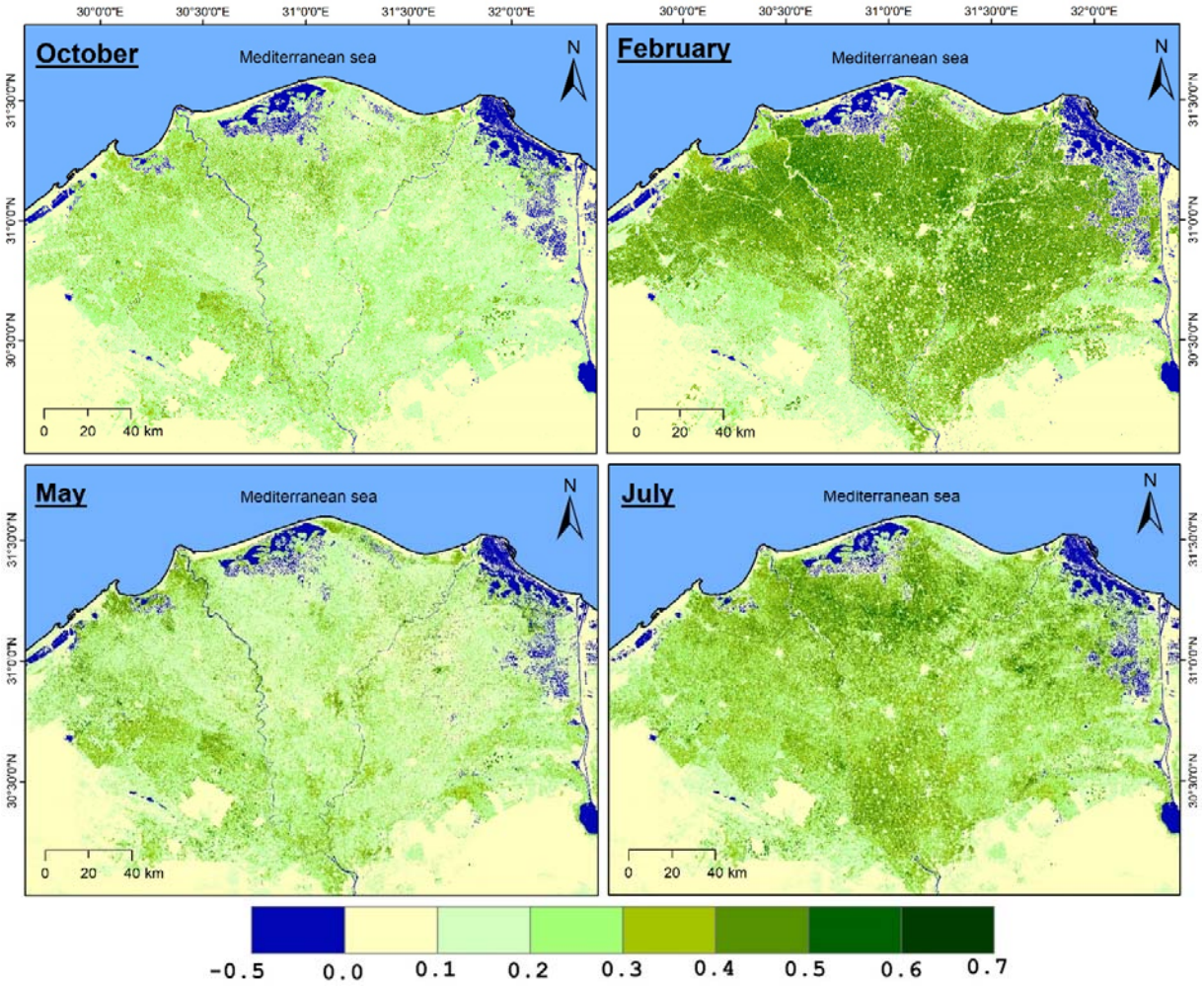

Fig. 3. NDVI for four seasons during 2017-2018, showing preparation and growth of winter crops (October, February) and summer crops (May, July) respectively.

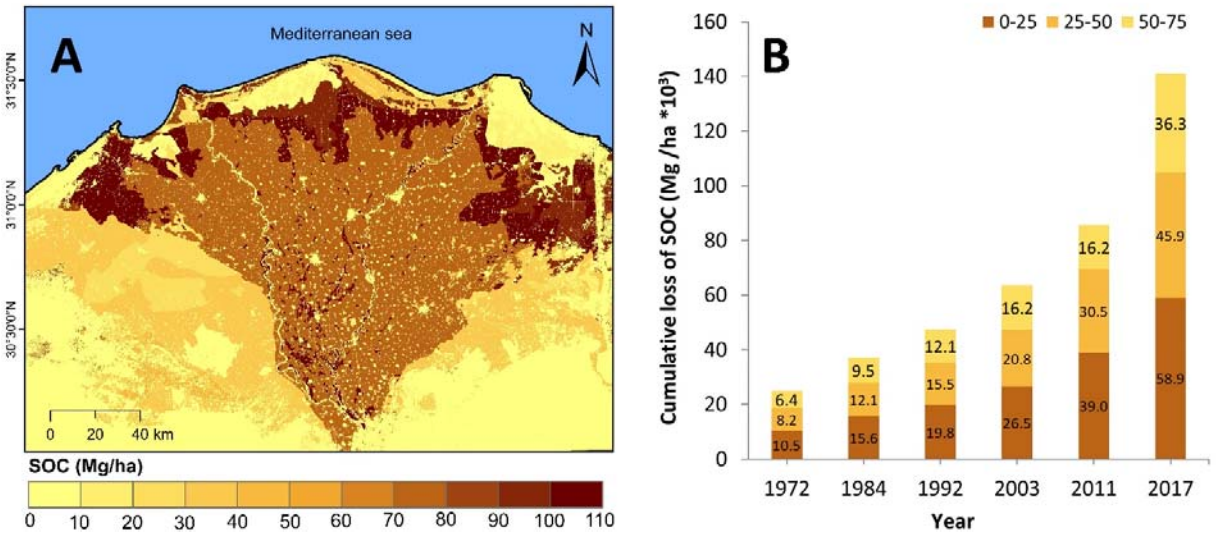

Fig. 4. Soil organic carbon (SOC) in Nile Delta. A) total SOC stock in Nile delta for a depth 0-75 cm (Mg ha^{-1}) in 2017; B) cumulative loss of SOC due to urbanisation over 45 years, split by soil depth.

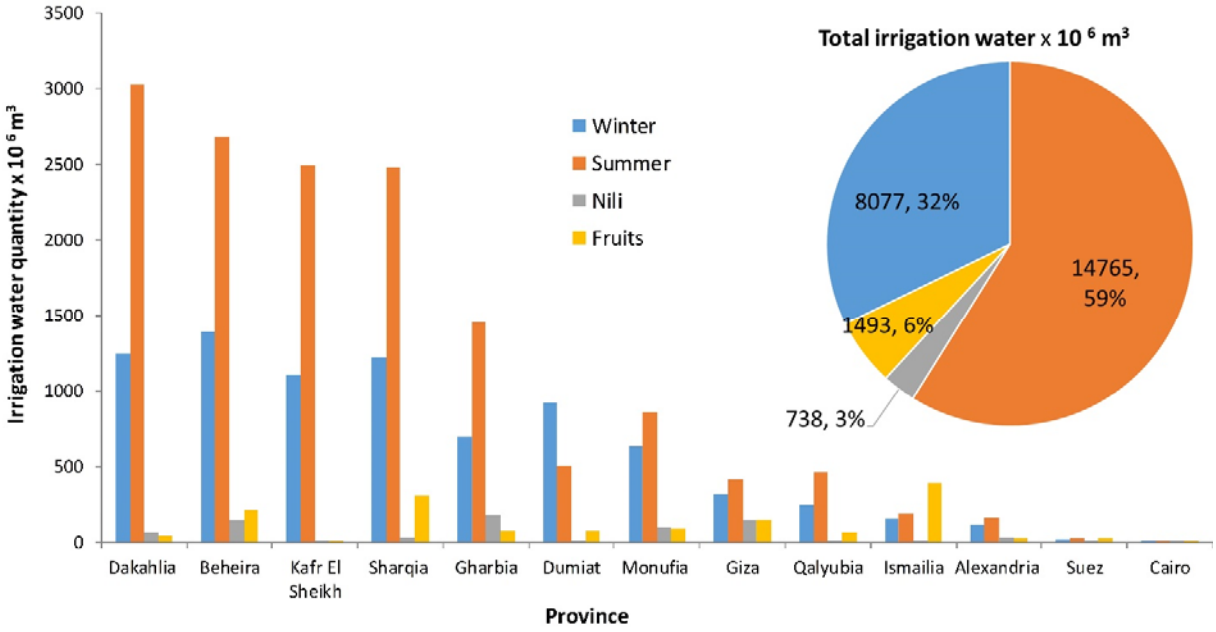

Fig. 5. Irrigation water use in delta governorates, by crop season, in 2015. Pie chart shows overall water quantity and proportion by crop season.

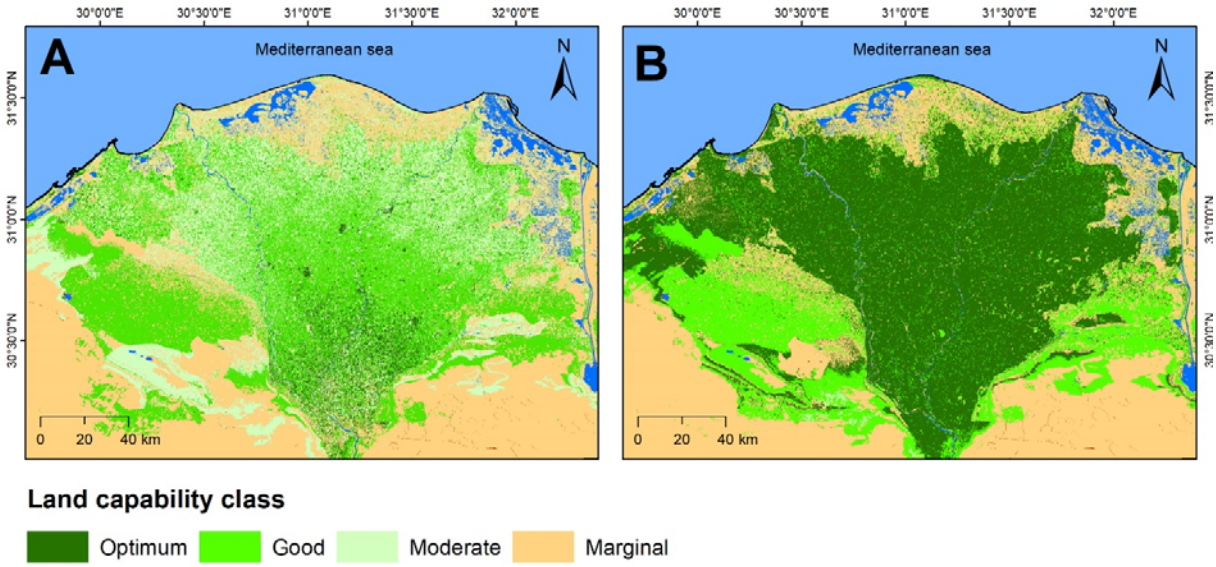

Fig. 6. Land capability classification under A) current situation and B) the soil improvement scenario

Supplementary Figures and Tables

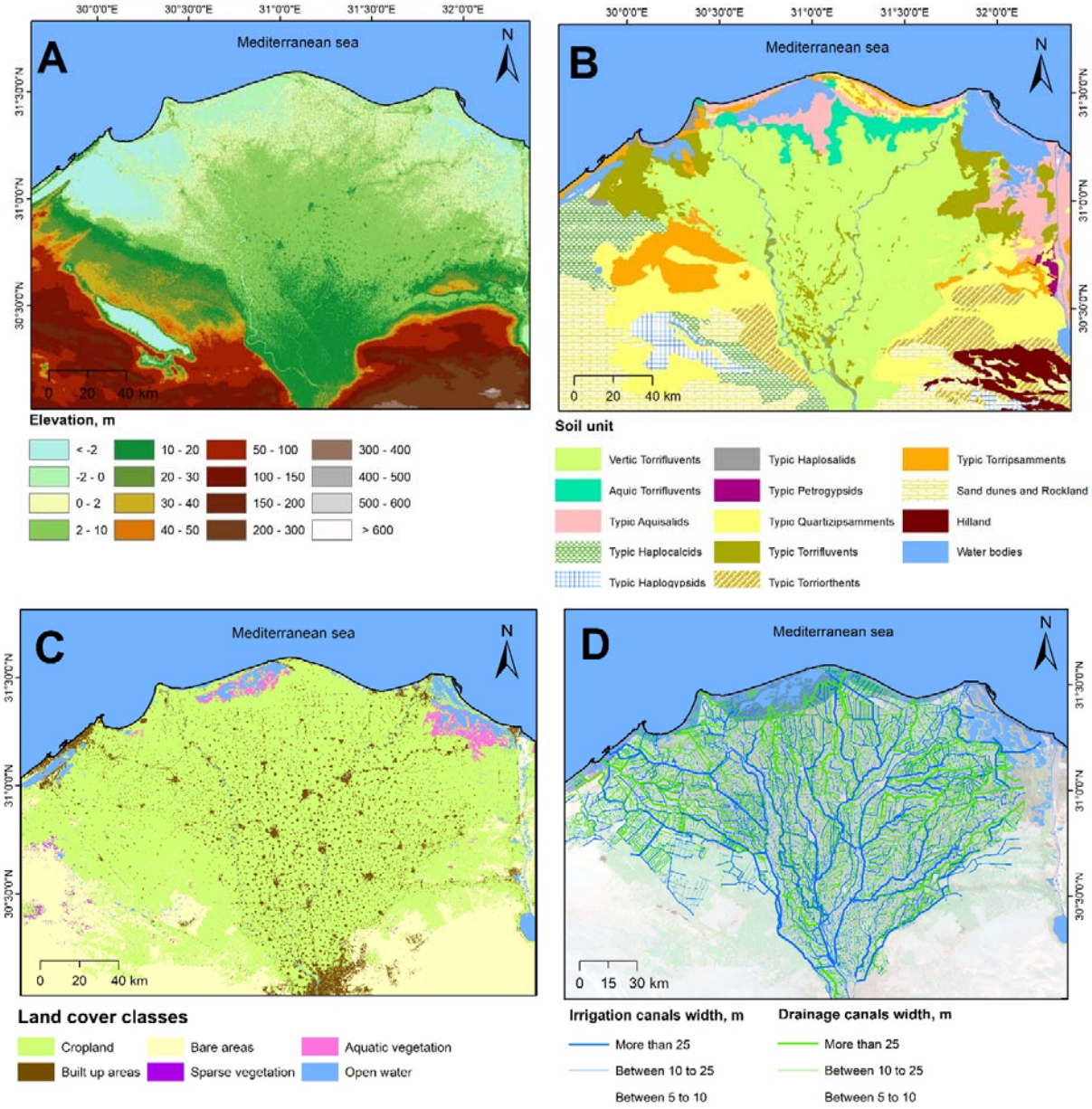

Fig. S1. Elevation (A), Soil type (B), Irrigation and drainage canal (C), Main Land cover classes (D).

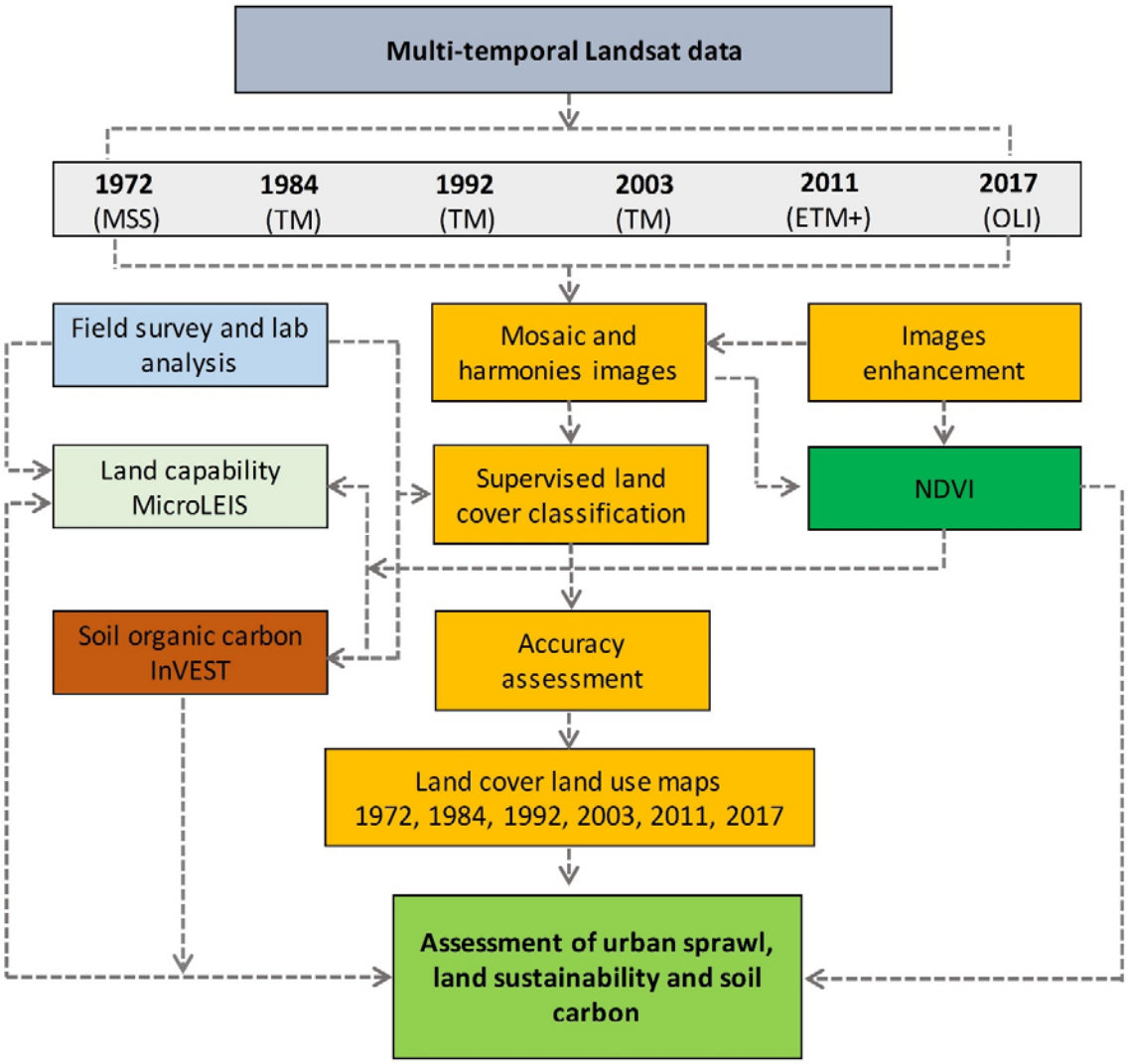

Fig. S2. Schematic diagram of the overall methodology.

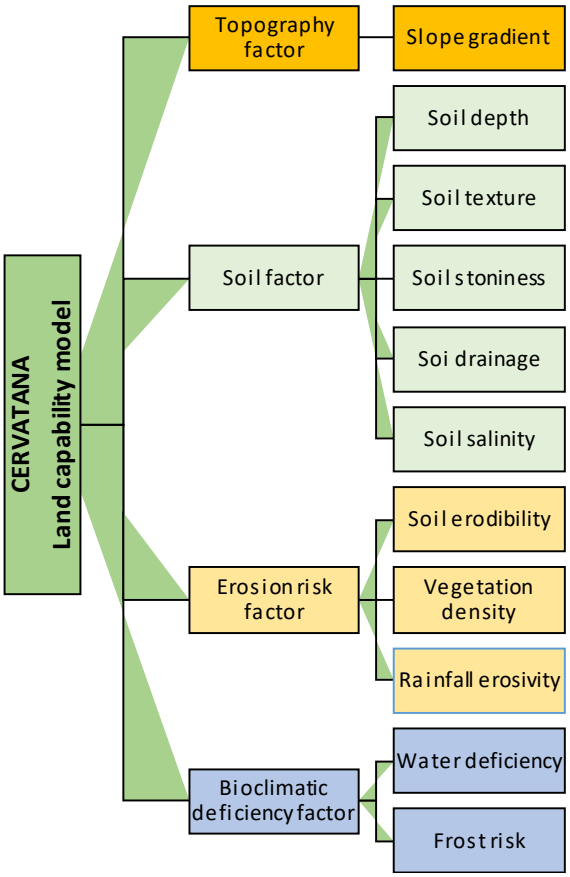

Fig. S3. Scheme for the Cervatana-MicroLEIS DSS Land capability model.

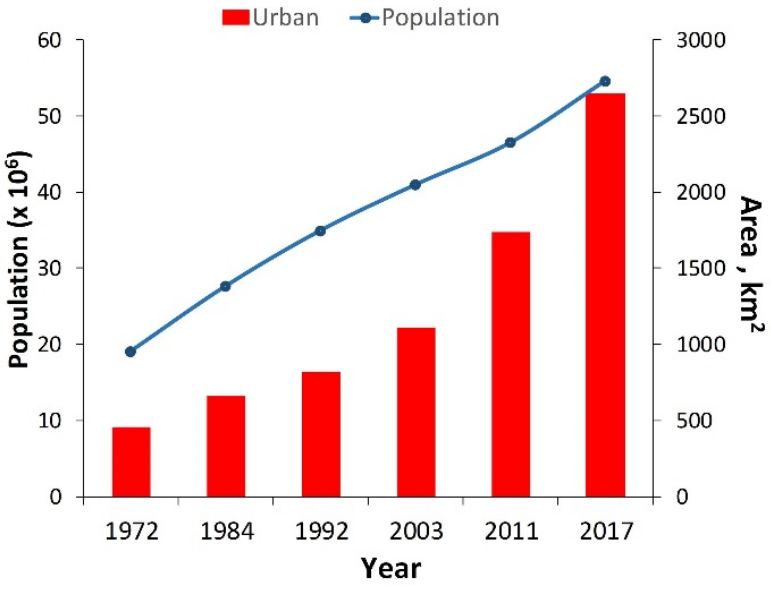

Fig. S4. Change in urban area (km^2) and population over the last 45 years in the Nile delta.

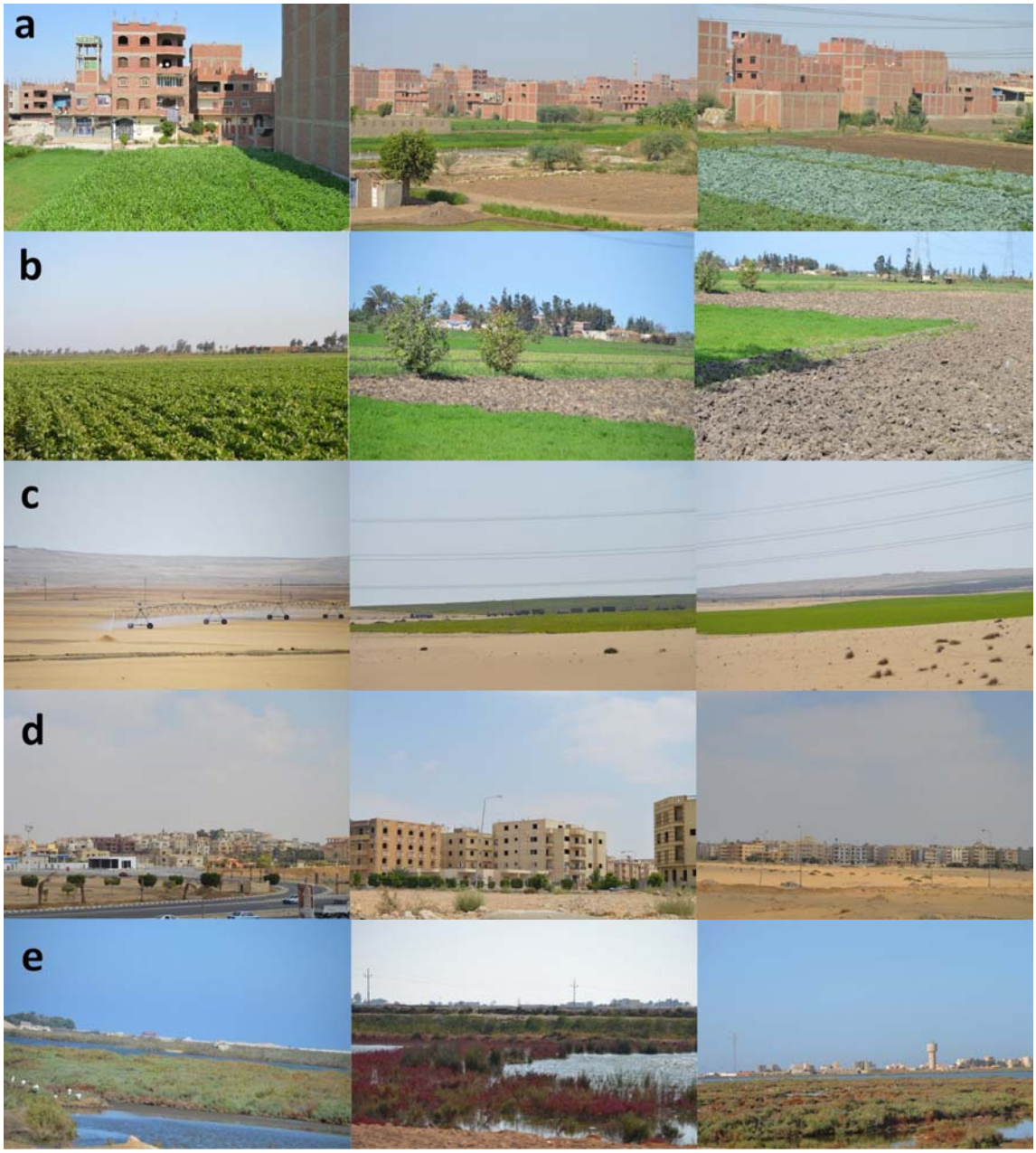

Fig. S5. Major land covers in Nile Delta. a, built up areas on the fertile soil; b, high capable agriculture lands; c, new cultivated land; d, new urban areas in marginal lands; e, water bodies and aquatic vegetation in the northern lakes of Nile Delta.

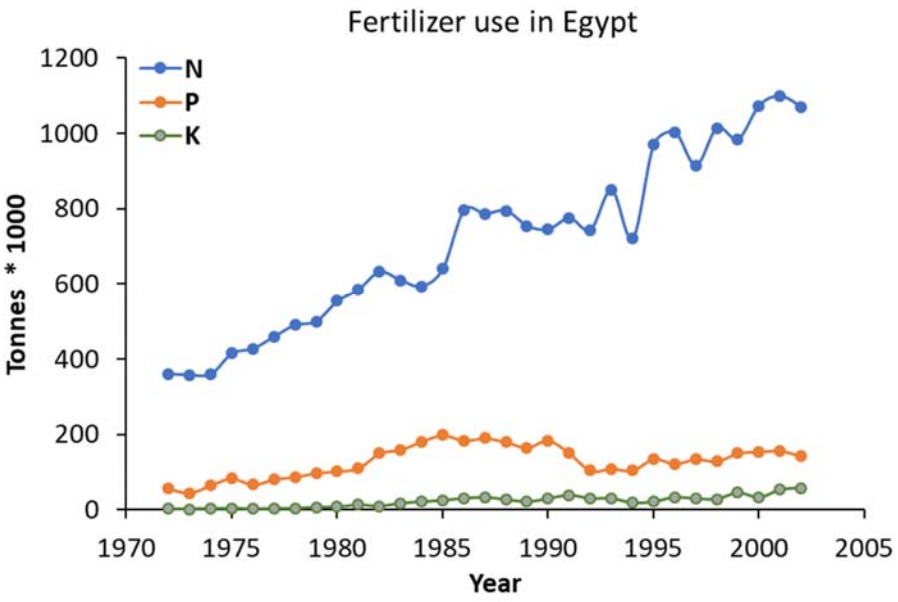

Fig. S6. The huge increment of nitrogen (N), phosphorous (P), and potassium (K) fertilizers in Egypt during the 1972 to 2002. Adapted from www.fao.org/faostat, 2019.

Table S1. Multi-temporal satellite data specification of the collected images for the studied dates. Different dates used within a month to obtain cloud-free imagery; the present data were used for Fig.3.

Acquisition date		Landsat Scene ID	Path /Row	Spacecraft / Sensor
1972	Octubre 5	LM11890381972279AAA05	189/38	Landsat 1 / MSS
	Octubre 5	LM11890391972279AAA05	189/39	
	August 31	LM11900381972244AAA04	190/38	
	August 31	LM11900391972244AAA04	190/39	
	Sept. 19	LM11910381972263AAA04	191/39	
	Sept.19	LM11910391972263AAA04	191/39	
1984	May 31	LT51760381984152FUI00	176/38	Landsat 5 / TM
	May 31	LT51760391984152FUI00	176/39	
	June 7	LT51770381984159XXX09	177/38	
	June 7	LT51770391984159XXX03	177/39	
1992	August 9	LT51760381992222RSA00	176/38	Landsat 5 / TM
	August 9	LT51760391992222RSA00	176/39	
	August 16	LT51770381992229RSA01	177/38	
	August 16	LT51770391992229RSA01	177/39	
2003	July 7	LT51760382003188MTI01	176/38	Landsat 5 / TM
	July 7	LT51760392003188MTI01	176/39	
	June 28	LT51770382003179MTI02	177/38	
	June 28	LT51770392003179MTI02	177/39	
2011	July 21	LE71760382011202ASN00	176/38	Landsat 7 / ETM+
	July 21	LE71760392011202ASN00	176/39	
	July 28	LE71770382011209ASN00	177/38	
	July 28	LE71770392011209ASN00	177/39	
2017	June 27	LC81760382017178LGN00	176/38	Landsat 8 / OLI
	June 11	LC81760392017162LGN00	176/39	
	June 2	LC81770382017153LGN00	177/38	
	June 2	LC81770392017153LGN00	177/39	

Table S2. Information about the collected Landsat 8 OLI images that used to obtain NDVI for different studied months during 2017, and 2018. The present data were used for Fig.4.

Acquisition date	Landsat Scene ID	Path / Row
October 17, 2017	LC81760382017290LGN00	176 / 38
October 1, 2017	LC81760392017274LGN00	176 / 39
October 24, 2017	LC81770382017297LGN00	177 / 38
October 8, 2017	LC81770392017281LGN00	177 / 39
February 22, 2018	LC81760382018053LGN00	176 / 38
February 2,2018	LC81760392018037LGN00	176 / 39
March 1, 2018	LC81770382018060LGN00	177 / 38
February 13, 2018	LC81770392018044LGN00	177 / 39
June 27,2017	LC81760382017178LGN00	176 / 38
June 27,2017	LC81760392017178LGN00	176 / 39
July 4, 2017	LC81770382017185LGN00	177 / 38
July 4, 2017	LC81770392017185LGN00	177 / 39
May 5, 2017	LC81760382017146LGN00	176 / 38
May 26, 2017	LC81760392017146LGN00	176 / 39
June 2, 2017	LC81770382017153LGN00	177 / 38
June 2, 2017	LC81770392017153LGN00	177 / 39

Table S3. Features of the used Landsat MSS, TM, ETM+ and OLI satellite images. NIR, Near Infrared; SWIR, Shortwave Infrared; TIR, Thermal infrared.

Landsat 1 MSS			Landsat 5 TM			Landsat 7 ETM+			Landsat 8 OLI		
Band	**Spatial resol. (m)**	**Wavelength (µm)**	**Band**	**Spatial resol. (m)**	**Wavelength (µm)**	**Band**	**Spatial resol. (m)**	**Wavelength (µm)**	**Band**	**Spatial resol. (m)**	**Wavelength (µm)**
B 4-Green	60 [I]	0.5-0.6	B 1-Blue	30	0.45-0.52	B 1-Blue	30	0.45-0.52	B 1- Ultra Blue	30	0.43 - 0.45
B 5-Red	60 [I]	0.6-0.7	B 2-Green	30	0.52-0.60	B 2-Green	30	0.53-0.61	B 2-Blue	30	0.45 - 0.51
B 6-NIR	60 [I]	0.7-0.8	B 3-Red	30	0.63-0.69	B 3-Red	30	0.63-0.69	B 3-Green	30	0.53 - 0.59
B 7-NIR	60 [I]	0.8-1.1	B 4-NIR	30	0.76-0.90	B 4-NIR	30	0.78-0.90	B 4-Red	30	0.64 - 0.67
-	-	-	B 5-SWIR 1	30	1.55-1.75	B 5-SWIR 1	30	1.55-1.75	B 5-NIR	30	0.85 - 0.88
-	-	-	B 6-Thermal	120 (30) [II]	10.40-12.50	B 6-Thermal	60 (30) [III]	10.40-12.50	B 6- SWIR 1	30	1.57 - 1.65
-	-	-	B 7-SWIR 2	30	2.08-2.35	B 7-SWIR2	30	2.09-2.35	B 7- SWIR 2	30	2.11 - 2.29
-	-	-	-	-	-	B 8-Panchr.	30	0.52-0.90	B 8-Panchc.	15	0.50 - 0.68
-	-	-	-	-	-	-	-	-	B 9-Cirrus	30	1.36 - 1.38
-	-	-	-	-	-	-	-	-	B 10-TIR 1	100 (30) [IV]	10.60 - 11.19
-	-	-	-	-	-	-	-	-	B 11-TIR 2	100 (30) [IV]	11.50- 12.51

[I] Original MSS pixel size was 79 x 57 meters; but are resampled to 60 meters.

[II] TM Band 6 was acquired at 120-meter resolution, but have been resampled to 30-meter pixels.

[III] ETM+ Band 6 is acquired at 60-meter resolution, but have been resampled to 30-meter pixels.

[IV] TIRS bands are acquired at 100m resolution, but have been resampled to 30 m in the delivered data product.

Source: http://landsat.usgs.gov.

Table S4. Confusion matrices, overall accuracies and Kappa coefficients for each studied date of the classified images.

Studied date		Reference Data						
		Cultivated land	Urban	Bare land	Aquatic vegetation	Water bodies	Total	User's Accuracy
Classified Data 1972	Cultivated land	293	37	0	7	3	340	86.2
	Urban	1	245	1	0	0	247	99.2
	Bare land	5	19	299	2	2	327	91.4
	Aquatic vegetation	0	0	0	90	1	91	98.9
	Water bodies	0	0	0	1	94	95	98.9
	Total	300	300	300	100	100	1100	
	Producer's Accuracy	97.7	81.7	99.7	90.0	94.0		
	Overall Accuracy, %							**92.8**
	Kappa Coefficient							**0.90**
1984	Agriculture	298	29	6	10	2	345	86.4
	Urban	0	270	7	0	0	277	97.5
	Bare	2	1	283	0	2	288	98.3
	Aquatic	0	0	4	90	0	94	95.7
	Water bodies	0	0	0	0	96	96	100.0
	Total	300	300	300	100	100	1100	
	Producer's Accuracy	99.3	90.0	94.3	90.0	96.0		
	Overall Accuracy, %							**94.3**
	Kappa Coefficient							**0.92**
1992	Cultivated land	300	12	15	3	0	330	90.9
	Urban	0	279	11	0	0	290	96.2
	Bare land	0	9	274	0	0	283	96.8
	Aquatic vegetation	0	0	0	95	0	95	100.0
	Water bodies	0	0	0	2	100	102	98.0
	Total	300	300	300	100	100	1100	
	Producer's Accuracy	100.0	93.0	91.3	95.0	100.0		
	Overall Accuracy, %							**95.3**
	Kappa Coefficient							**0.94**
2003	Cultivated land	300	4	14	1	1	320	93.8
	Urban	0	286	1	0	0	287	99.7
	Bare land	0	10	285	0	0	295	96.6
	Aquatic vegetation	0	0	0	99	1	100	99.0
	Water bodies	0	0	0	0	98	98	100.0
	Total	300	300	300	100	100	1100	
	Producer's Accuracy	100.0	95.3	95.0	99.0	98.0		
	Overall Accuracy, %							**97.1**
	Kappa Coefficient							**0.96**
2011	Cultivated land	297	3	16	0	0	316	94.0
	Urban	0	291	7	0	0	298	97.7
	Bare land	3	6	275	3	3	290	94.8
	Aquatic vegetation	0	0	1	95	0	96	99.0
	Water bodies	0	0	1	2	97	100	97.0
	Total	300	300	300	100	100	1100	
	Producer's Accuracy	99.0	97.0	91.7	95.0	97.0		
	Overall Accuracy, %							**95.9**
	Kappa Coefficient							**0.95**
2017	Cultivated land	296	2	15	0	0	313	94.6
	Urban	2	298	11	0	0	311	95.8
	Bare land	2	0	269	0	0	271	99.3
	Aquatic vegetation	0	0	5	99	1	105	94.3
	Water bodies	0	0	0	1	99	100	99.0
	Total	300	300	300	100	100	1100	
	Producer's Accuracy	98.7	99.3	89.7	99.0	99.0		
	Overall Accuracy, %							**96.5**
	Kappa Coefficient							**0.95**

Table S5. Mean values of Soil organic carbon stock (Mg/ha) per soil types for different soil depths.

	SOC (Mg/ha)			
Taxonomic unit	**0-25 cm**	**25-50 cm**	**50-75 cm**	**0-75 cm**
Aquic Torrifluvents	42.76	35.3	27.68	105.74
Typic Aquisalids	35.66	33.02	25.17	93.85
Typic Haplocalcids	16.45	11.82	11.65	39.92
Typic Haplogypsids	25.72	12.39	10.3	48.41
Typic Haplosalids	34.1	29.2	21.1	84.40
Typic Petrogypsids	11.005	4.459	1.1213	16.59
Typic Quartzipsamments	16.58	11.13	9.74	37.45
Typic Torrifluvents	42.13	33.99	24.64	100.76
Typic Torriorthents	15.5	10.38	14	39.88
Typic Torripsamments	10.845	7.94	6.06	24.85
Vegetation aquatic	34.1	29.2	21.1	84.40
Vertic Torrifluvents	30.29	23.5	18.463	72.25

Table S6. Urban expansion rate (UER, $km^2\ yr^{-1}$) over the soil units during the studied dates. I, 1972-1984; II,1984 -1992; III,1992-2003; IV,2003-2011; V, 2011-2017.

	Urbanisation period				
Soil map unit	**I**	**II**	**III**	**IV**	**V**
Vertic Torrifluvents	9.53	6.78	14.25	33.86	59.01
Typic Torrifluvents	1.28	1.99	2.00	5.70	13.12
Typic Quartizipsamments	0.97	2.84	2.85	10.38	18.73
Typic Torriorthents	0.37	0.33	0.85	3.03	6.86
Typic Petrogypsids	0.11	0.34	0.33	0.70	0.61
Typic Haplogypsids	0.05	0.08	0.20	0.36	2.25
Typic Aquisalids	0.56	3.14	1.26	4.17	6.48
Typic Torripsamments	0.29	1.32	0.85	2.78	10.01
Typic Haplosalids	0.10	0.12	0.28	0.93	2.15
Typic Haplocalcids	0.25	0.45	0.64	3.90	10.48
Aquic Torrifluvents	0.34	0.81	0.36	1.16	2.93
Hilland	0.09	0.17	0.20	1.33	2.03
Rock land	0.46	0.21	1.60	4.87	12.48

Table S7. Cumulative loss of SOC (Mg of carbon) for the various soil types at different soil depths.

	0-25 cm						25 -50 cm						50-75 cm					
Taxonomic unit	**1972**	**1984**	**1992**	**2003**	**2011**	**2017**	**1972**	**1984**	**1992**	**2003**	**2011**	**2017**	**1972**	**1984**	**1992**	**2003**	**2011**	**2017**
Typic Torrifluvents	1344	1987	2659	3488	5108	8255	1084	1603	2145	2814	4121	6660	786	1162	1555	2040	2040	4828
Typic Quartizipsamments	209	347	728	1170	2309	4036	140	233	489	786	1550	2710	122	204	428	688	688	2371
Typic Torriorthents	4	55	98	216	511	1102	3	37	66	145	342	738	4	50	88	195	195	995
Typic Petrogypsids	1	18	47	86	144	183	0	7	19	35	58	74	0	2	5	9	9	19
Typic Haplogypsids	12	8	25	61	75	386	6	4	12	29	36	186	5	3	10	24	24	155
Typic Aquisalids	48	254	1151	1578	2570	3843	45	235	1066	1461	2379	3559	34	179	812	1114	1114	2713
Typic Torripsamments	44	67	183	266	451	1069	32	49	134	195	330	783	24	38	102	149	149	597
Vertic Torrifluvents	8419	12206	13932	18337	25545	35674	6531	9470	10809	14227	19818	27677	5132	7440	8492	11177	11177	21745
Typic Haplosalids	28	70	103	202	443	875	24	60	88	173	379	749	17	43	64	125	125	542
Typic Haplocalcids	6	30	92	178	599	1581	4	22	66	128	431	1136	4	21	65	126	126	1120
Aquic Torrifluvents	346	509	786	924	1221	1914	285	420	649	763	1008	1580	224	330	509	598	598	1239
Total	**10460**	**15552**	**19803**	**26507**	**38976**	**58919**	**8155**	**12141**	**15542**	**20755**	**30454**	**45851**	**6352**	**9472**	**12130**	**16245**	**16245**	**36322**

Table S8. Total area in km^2 and % of land capability class. A; current situation; B, improvement scenario.

Class	A - Area		B - Area	
	km^2	%	km^2	%
Optimum	1601.6	3.9	17055.9	41.8
Good	12970.5	31.8	7989.4	19.6
Moderate	9871.0	24.2	267.2	0.7
Marginal	16362.2	40.1	15492.7	38.0
Total	**40805.3**	**100.0**	**40805.3**	**100.0**